Tutor/s

Dr. Joan Dosta Parras
Departament d'Enginyeria Química

Dr. César Alberto Valderrama Angel
Departament d'Enginyeria Química UPC

Grau en Enginyeria Química

Treball Final de Grau

Phosphorus recovery as hydroxyapatite (HAP) from urban wastewaters using nanofiltration and reverse osmosis brines.

Recuperació del fòsfor en forma d'hidroxiapatita (HAP) de les aigües residuals municipals fent servir salmorres procedents de nanofiltració i osmosi inversa.

Gádor Indra Hidalgo López

June 2014

Universitat de Barcelona

Dos campus d'excel·lència internacional
B:KC Barcelona Knowledge Campus
HUBC Health Universitat de Barcelona Campus

Primer de tot voldria agrair al meu tutor, el Dr. Joan Dosta Parras per donar-me la possibilitat de realitzar aquest Treball Final de Grau sobre aquest tema d'investigació pioner, així com per la seva tutoria, ja que ha estat per a mi un veritable mentor i model a seguir. Tanmateix voldria agrair al Dr. José Luis Cortina Pallás i al Dr. César Alberto Valderrama Angel, del departament d'Enginyeria Química de la UPC haver-me permès formar part del seu equip de recerca i dotar-me de medis i material per poder dur a terme aquesta investigació.

Voldria agrair al Dr. Joan Mata Álvarez per haver-me no només introduït sinó despertat un gran interès pel món del medi ambient i a tot el departament d'Enginyeria Química de la UB per la seva tasca de formació en l'àmbit de l'Enginyeria Química, sense els quals no podria haver realitzat aquest treball. Al meu tutor de grau Dr. Claudi Mans Teixidor, per la seva tasca durant aquests quatre anys. Per acabar, voldria agrair a la persona que em va introduir al món de la Química, transmetent els seus coneixements i la passió per aquesta ciència, Marta Segura i Fàbregas, gràcies. Per últim, agrair als familiars i amics pel seu recolzament, empatia i afecte.

REPORT

CONTENTS

1. SUMMARY

The recovery of phosphorus from wastewater appears to be the best option to ensure the recyclability of this product and save the fertiliser industry from losing its key element. Chemical precipitation is an effective method to obtain calcium phosphate in the form of hydroxyapatite (HAP), which can be applied to the soil as a fertiliser. In a Waste Water Treatment Plant (WWTP), the liquid effluent from the secondary clarifier is rich in phosphorus. This effluent can be introduced in an ion exchange unit that, when being regenerated, produces a solution with a concentration up to 1,000 mg PO_4^{3-}/L. This stream can undergo chemical precipitation thanks to the addition of calcium ions with alkaline media. Concentrate or reject stream obtained from nanofiltration (NF) or reverse osmosis (RO) processes can be used as a source of calcium, valorising both wastewater and brines.

A laboratory scale study is conducted using a semi continuous stirred batch reactor to precipitate phosphate of a solution that simulates the regenerated stream in the ion-exchange unit of a WWTP, using nanofiltration and reverse osmosis brines with and without Mg^{2+} at different pH. Results indicate that the presence of Mg^{2+} enhances phosphate removal, but does not stimulate HAP formation. The conditions that achieve higher phosphate removal are the NF and RO brines with Mg^{2+} at pH=10.5, representing almost a 100 % of removal. In all four types of brines, higher removal is obtained at pH=10.5. The type of brine does not have as much effect as other factors such as the presence of Mg^{2+} or pH. In less time, NF brine removes the same amount of phosphate from the solution than RO brine when there is Mg^{2+}.

Hydroxyapatite has been found at the two studied pH using both nanofiltration and reverse osmosis brines without magnesium. It has also been found crystalline halite in these same situations where HAP has been found. At pH=12, using reverse osmosis reject with Mg^{2+} only crystalline halite has been found.

2. RESUM

La recuperació del fòsfor de les aigües residuals es posiciona com la millor opció per assegurar la reutilització d'aquest producte i salvar la indústria dels fertilitzants de la pèrdua del seu element clau. La precipitació química és un mètode eficaç per obtenir fosfat de calci en forma d'hidroxiapatita (HAP), que es pot aplicar al sòl com a fertilitzant. En una Estació Depuradora d'Aigües Residuals (EDAR), l'efluent líquid procedent del sedimentador secundari és ric en fòsfor. Aquest efluent pot ser introduït a una unitat d'intercanvi iònic que, en ser regenerat, produeix una solució amb una concentració de fins a 1000 mg PO_4^{3-}/L. Aquest corrent pot sotmetre's a una precipitació química gràcies a l'addició de ions calci en medi bàsic. La corrent concentrada procedent de processos de nanofiltració (NF) o d'osmosi inversa (OI) es pot utilitzar com una font de calci, valoritzant alhora les aigües residuals i les salmorres.

S'ha dut a terme un estudi a escala de laboratori fent servir un reactor tanc agitat semi continu per precipitar el fosfat d'una solució que simula la corrent regenerada en la unitat d'intercanvi iònic d'una EDAR, fent servir salmorres sintètiques amb o sense presència de Mg^{2+} a diferent pH. Els resultats indiquen que la presència de Mg^{2+} millora l'eliminació de fosfat, però no promou la formació de HAP. Les condicions que ens permeten obtenir més eliminació del fosfat són les salmorres de NF i OI amb Mg^{2+} a pH=10,5, representant gairebé un 100% de eliminació. En els quatre tipus de salmorra, s'ha obtingut una eliminació més alta a pH=10,5. El tipus de salmorra no té un efecte tan pronunciat com altres factors com la presencia de Mg^{2+} o el pH. En un menor temps, la salmorra procedent de NF elimina la mateixa quantitat de fosfat de la solució que la procedent de OI quan hi ha Mg^{2+}.

S'ha trobat hidroxiapatita cristal·lina en els dos pHs estudiats utilitzant les salmorres sense magnesi tant de nanofiltració com d'osmosi inversa. També s'ha trobat halita cristal·lina en aquests casos on s'hi ha trobat HAP. A pH=12, usant el concentrat de osmosi inversa amb Mg^{2+} només s'ha trobat halita cristal·lina.

3. INTRODUCTION

At this stage phosphorus will be introduced as a chemical element and as an important substance present in nature and its multiple applications. Its effect will be discussed when the natural equilibrium is altered, such as the problem of eutrophication and its ecological impact and the effects on the population. Phosphate recovery from wastewater appears to be the best option to ensure the recyclability of this product and save the fertiliser industry from losing its source compound. Chemical precipitation is an effective method of obtaining calcium phosphate in a form which can be applied to the soil as a fertiliser.

3.1. PHOSPHORUS, A KEY ELEMENT

Phosphorus is a nonmetallic chemical element with symbol P and atomic number 15. Elemental phosphorus exists in several forms, or allotropes, but due to its high reactivity, it is found in nature in its maximally oxidised state, as inorganic phosphate in rocks. The most common phosphorus allotropes are white phosphorus and red phosphorus, but there are some more such as violet or black. Although they are all phosphorus, they have remarkable different properties.

Figure 1.Left to right: white phosphorus, red (particles), red (solid), violet phosphorus

(Peter Krimbacher, 25/5/2014 via Wikimedia Commons, Creative Commons Attribution)

Phosphorus is a rare element in the lithosphere, composing a 0.1% of the total elemental composition, with an average concentration of 1180 ppm (Fairbridge, 1972; Taylor, 1964).

It is an indispensable element for the normal biological functioning of living beings, as it is necessary for a wide range of cellular functions.

3.1.1. Natural sources

Phosphorus is present in mineral sources mainly in the form of phosphate. Phosphate rocks are formed by apatites (fluorapatite ($Ca_5(PO_4)_3F$) or carbonate fluorapatite ($Ca_5(PO_4,CO_3)_3F$)) which is the principal industrial mineral in the rock from which the phosphorus is extracted.

Figure 2. Phosphate rock mine.

(Jason Parker-Burlingham, 25/5/2014 via Wikimedia Commons, Creative Commons Attribution)

Sedimentary marine phosphorite deposits, also called phosphorites and carbonatites and alkaline igneous rocks are also natural phosphorus sources.

Guano, which is bird excrement, contains a great amount of phosphate, and is present in great amount in tropical islands of South America. Due to the massive exploitation during the nineteenth century to be used as a fertilizer, these phosphorus deposits have been exhausted.

3.1.2. Applications

Phosphoric acid, organophosphorus compounds for use in plasticizers, flame retardants, pesticides, extraction agents, water treatment (Greenwood, Earnshaw, 1997), metallurgical applications, matches and detergents are some of the applications of phosphorus in some of its chemical forms.

The main application of extracted phosphorus is its use as artificial fertiliser, as nutrients are necessary for the plant growth. Although ground naturally contains the necessary elements for food production, not all the soils have the same quality, needing some extra addition of minerals such as phosphorus, nitrogen or potassium.

Since the mid-20th century population growth concomitant with increased food demand and urbanisation have resulted in a dramatic increase in the use of mined phosphate rock as compared to other P sources. Phosphorus demand for food production is about 90% of the total (Smit et al., 2009).

The use of fertilisers plays a critical role in increasing yields but some estimates indicate that existing phosphate rock reserves may be depleted within 50–120 years (Cordell et al., 2009; Fixen, 2009; Smit et al., 2009).

Humankind has increased the rate of phosphorus cycling on Earth by four times, mainly due to agricultural fertiliser production and application. Between 1950 and 1995, an estimated 600,000,000 tonnes of phosphorus were applied to Earth's surface, primarily on croplands (Carpenter et al., 1998). Annual application of 40–120 kg mineral P_2O_5 fertilizer per ha (approximately 18–52 kg P/ha) are required to maintain agricultural productivity (Ott, Rechberger, 2012).

3.1.3. Wastewaters and the problem of eutrophication

Wastewaters contain high concentrations of nutrients due to their nature. Living beings, although processing food, do not use 100% of it, and therefore phosphorus and nitrogen are left in the organic residues that form the excreta.

On the other hand, industrial wastewaters also have high amounts of nutrients, especially those obtained in certain industries such as fertilisers, detergent and alimentary industries and farming in general, due to the gathering effect of water when passing through an area. This collects organic matter, fertilisers and other substances richly loaded with P and N.

Aquatic systems have an ideal stoichiometric Si:N:P nutrient ratio 16:16:1 which can be easily altered if are poured untreated urban or industrial wastewaters (Redfield, 1958).

Excessive influx of phosphorus and/or nitrogen (usually in form of phosphates and nitrates) into natural water effluents causes algae to overgrow due to the excessive amount of nutrients. This is called eutrophication, or hypertrophication. This also causes oxygen in the water to

diminish due to the O_2 consumed by bacteria when decomposing dead algae. Without oxygen, fish and shellfish cannot survive. This fauna loss affects directly human population, as it alters the food chain, decreasing the supply of food for people or other animals such as bears or foxes.

Another problematic issue is the water treatment of these eutrophicated reservoirs to produce drinking water. Health problems can appear if this altered water is consumed, due to the presence of harmful algal blooms (HABs), which are algal bloom events involving toxic or otherwise harmful phytoplankton such as dinoflagellates of the genus Alexandrium and Karenia, or diatoms of the genus Pseudo-nitzschia (Kirkpatrick et al., 2004). Such blooms often take on a red or brown hue and are known colloquially as red tides.

3.2. PHOSPHORUS REMOVAL FROM WASTEWATERS

There are many different techniques to remove the P in the wastewater such as chemical precipitation, adsorption, reverse osmosis, biological removal, and constructed wetlands.

When treating wastewater effluents, there are points in the WWTPs (Waste Water Treatment Plants) where the P concentration is higher, enabling a feasible separation and thus recovering process.

In the figure 3 there is a scheme of the secondary treatment in a WWTP and the equipment necessary to remove and recover the phosphorus from the water effluent.

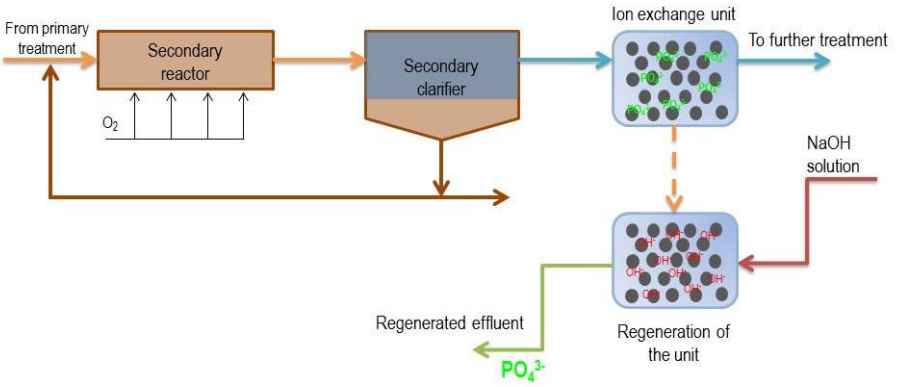

Figure 3. Waste Water Treatment Plant scheme.

After the secondary clarifier, the water effluent can be treated with an ion exchange resin, to capture the phosphate ions from the solution. By this method, the water can continue its treating process in the WWTP as this treatment has decreased its phosphate concentration. If a larger removal of the phosphate is necessary, further treatments can be applied until the effluent is apt to be incorporated to natural water effluents.

When the exchange resin is saturated, it is regenerated using the ideal solution to replace PO_4^{3-} anions with other anions, so that the phosphate is released and can be recovered. The ideal solution will depend on the type of resin used to retain the phosphate in this treatment. In this scheme, NaOH is used to substitute PO_4^{3-} ions with OH^- from the basic solution. With this method, up to 1,000 mg PO_4^{3-}/L can be found in the obtained regenerated effluent. This stream is then treated to recover the phosphate by chemical precipitation.

3.2.1. Chemical precipitation

The main process used in WWTPs for P removal from wastewater is chemical precipitation with Fe, Al or Ca, which involves the addition of cationic salts to water containing phosphate, to produce a precipitation of insoluble phosphate complexes, and allow the separation of precipitates from the aqueous phase. Although some precipitates containing phosphorus can be recycled as fertilisers through land application, this application is impossible when the salts obtained contain metals which are not compatible with agricultural crops, as it would be a serious health problem. Phosphate precipitated as Fe or Al salts is unrecoverable for potential processing into fertilizer (Donnert, Salecker, 1999).

Phosphorus recovered from wastewater or leachates of P-containing solids may be further utilised in industrial or agricultural applications. In particular, where P is sorbed to a mineral-based material or precipitated as a phosphate mineral the resultant solid phase may be suitable for use as a slow-release P fertilizer. The use of P-containing mineral-based materials as soil amendments may be particularly advantageous where additional agronomic benefits are conferred, such as improved soil moisture holding capacity or the provision of other essential plant nutrients (Wendling et al., 2013).

Recovering (not only removing) the phosphorus from wastewaters has two elemental benefits: it avoids the eutrophication problem and decreases the amount of phosphate extracted from mineral sources by reusing the P which has already been mined.

Magnesium and calcium phosphates offer a plausible solution to recover phosphorus by chemical precipitation.

3.2.1.1. Magnesium phosphates. Struvite

Research in the area of P recovery by chemical precipitation has largely focused on the recovery of struvite ($NH_4MgPO_4 \cdot 6H_2O$), particularly in the case of domestic wastewater treatment. Struvite has excellent properties as a slow release fertiliser without much risk to the environment (Bridger et al., 1962; Lunt et al., 1964).

3.2.1.2. Calcium phosphates. Hydroxyapatite

Hydroxyapatite (HAP) $Ca_5(PO_4)_3(OH)$ is a mineral of the apatite group. This apatite is a group of phosphate minerals which are characterised by having calcium and phosphate on their structure. Ca/P molar ratio determines the type of calcium phosphate, and consequently, its properties, such as solubility. Lower Ca/P molar ratios involve more soluble calcium phosphates. Hydroxyapatite is the most stable form of the calcium phosphates, and the least soluble.

The formula used to describe hydroxyapatite is $Ca_{10}(PO_4)_6(OH)_2$ due to the fact that the crystal unit cell includes two $Ca_5(PO_4)_3(OH)$. Its name describes the fact that the end member of the apatite group contains a hydroxyl group. These ions can be replaced by other anions, to form other minerals such as fluorapatite or chlorapatite.

Hydroxyapatite crystal is colorless or has a slightly coloration (brown, green or yellowish) if it has impurities, and pure powder is white.

The crystal structure of non-stoichiometric hydroxyapatite (common in nature) is hexagonal di-pyramidal (crystal class), which is included in the hexagonal crystal system and crystal family. Hydroxyapatite hardness is 5 according to Mohs scale of mineral hardness. There is another type, which is monoclinic, more stable and corresponds to stoichiometric HAP (Leventouri, 2006).

It has attracted much attention as a substitute material for damaged teeth or bones over the past several decades, because of its crystallographical and chemical similarity with various calcified tissues of vertebrates (Suchanek W., Yoshimura M., Mater J., 1998), (Hench L.L., 1991). HAP ceramics does not exhibit any cytotoxic effects. It shows excellent biocompatibility with hard tissues and also with skin and muscle tissues. Moreover, HAP can directly bind to the

bone, allowing posterior bone growth. Hydroxyapatite is the main mineral constituent of teeth enamel.

3.2.1.3. HAP Precipitation mechanism

Supersaturation is the driving force for nucleation and crystal growth, which are the two events of the precipitation mechanism, and they both take part simultaneously during a large part of the time.

Nucleation needs supersaturation and minuscule solid particles: seed crystal or nuclei, which act as starting point to which other particles add and form a stable aggregate that will continue growing.

Nucleation can be primary or secondary. In **primary nucleation**, the formation of the new solid phase is not influenced by the presence of the solid phase being formed. This type of nucleation can be either homogeneous or heterogeneous.

Homogeneous nucleation. It is initiated by collisions between two molecules, which sometimes result in stable embryos (small number of molecules), which can keep growing.

Heterogeneous nucleation. The nucleation process is usually enhanced by the presence of impurity particles, ions or foreign surfaces. These lower the nucleation energy barrier.

Secondary nucleation is induced by the presence of macroscopic crystals of the precipitate.

Crystal growth. Solute molecules from the supersaturated solution adhere to the crystal created during nucleation.

HAP formation, which is a thermodynamically stable phase, is preceded by the formation of less stable (metastable) phases with higher energy (kinetically favoured) like amouphous calcium phosphate or octacalcium phosphate, depending on the experimental conditions. The precipitation reaction should be carefully controlled if no other salts want to be obtained.

To obtain HAP by chemical precipitation, the Ca/P molar ratio should be the stoichiometric one 1.67. This determines the initial phosphate and calcium concentration in the reactor to achieve this specific calcium phosphate. Non-stoichiometric products are usually obtained when executing chemical precipitation in a stirred batch reactor. To overcome homogeneity problems in the distribution of supersaturation in the reactor, semi-batch configuration has been used.

Previous studies in the Chemical Engineering department of Universitat Politècnica de Catalunya (UPC) have found the best conditions to recover phosphorus precipitating hydroxyapatite using a stirred batch reactor operating at room temperature. $CaCl_2$ solution was added very slowly to enhance the formation of HAP. As the flow rate is smaller, more HAP is formed, but the experiment is too long. The adequate stirring speed is 250-260 rpm and the calcium flow rate 0.3 mL/min.

As buying $CaCl_2$ to recover phosphorus in the WWTPs scale is very expensive, the concentrate of nanofiltration or reverse osmosis processes can be used as a calcium source, revaluing both waste waters and brines.

4. JUSTIFICATION AND OBJECTIVES

Phosphorus recovery is necessary to prevent its loss through wastewater streams and sewage sludge landfill disposal. By recovering the phosphorus from wastewaters as calcium phosphate, a fertiliser can be obtained, while eutrophication and finite phosphorus rock reserves problems are overcome.

For this reason, the current study focuses on the recovery of phosphate from the regenerated effluent through the chemical precipitation of hydroxyapatite using a synthetic solution of salts to simulate nanofiltration and reverse osmosis brines. In this way, it can be determined whether it is possible to obtain hydroxyapatite in the precipitated solid when there are other salts in the brine other than $CaCl_2$, as in real recycled brines.

More specifically, to reach this overall objective, several goals are pursued: to determine the effect of Mg^{2+}, pH and the type of brine in phosphate removal and the solid obtained; and to find the best conditions to obtain HAP.

5. MATERIALS AND METHODS

The experimental set up is schematised, as well as the types of brines and their components. The experimental procedure is detailed for further research using this methodology, and the analytical methods used to determine the amount of phosphate and characterise the obtained precipitate are here summarised.

5.1. EXPERIMENTAL SET UP

The prepared brine solution, thanks to a peristaltic pump (Gilson MINIPULS 3), will be continuously fed into the reactor at a flow rate of 0.3 mL/min when the experiment starts (see figure 4). Another pump (Cole-Parmer 7520-67 Masterflex Console Drive) will supply the necessary NaOH (1 M) to maintain the pH at the desired range, which is ±0.1 of the selected pH value. This pump is connected to a pH controller (Crison PH 28) which regulates the hydroxide supply depending on the pH detected by the pH probe (Mettler HA 405-DPA-SC-S8/225 Combination pH). The pH controller is configured at this point but the pump left disconnected to adjust the pH manually with NaOH 3 M at first to avoid diluting too much the initial 1,000 ppm phosphate solution. When the pH is near the correct value, the pump will be connected and the controller will adjust itself until the desired pH.

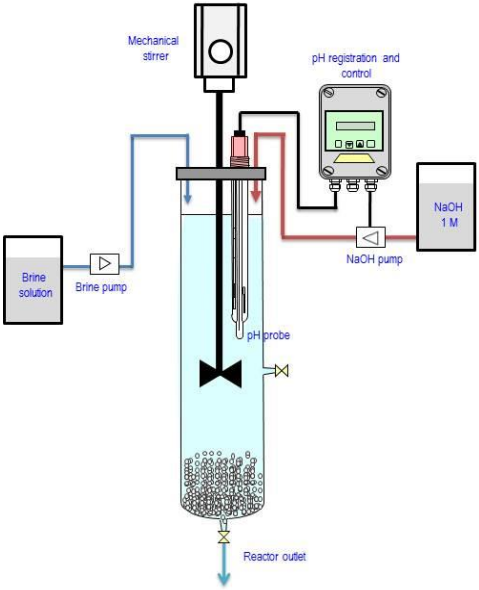

Figure 4. Experimental set up.

5.2. SYNTHETIC WASTEWATER AND BRINES

The **wastewater** used in the experiments is synthetic, prepared adding $NaH_2PO_4 \cdot H_2O$ to distilled water. See Appendix 1: Preparation of solutions.

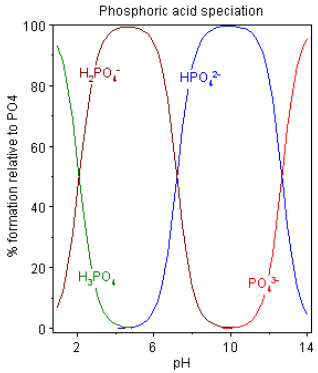

Figure 5. Phosphoric acid equilibrium.

High pH is used to promote PO_4^{3-} presence in the phosphoric acid equilibrium. See figure 5.

To prepare the **brines**, different salts are dissolved into 1 L of distilled water (Milli-Q is used to prepare solutions, from now on it will be referred to as distilled water) using a volumetric flask. Depending on the type of salts used, the brine will be a nanofiltration type or reverse osmosis type. The experiments take place using four types of brines, which are named A, B, C and D to distinguish them. The salts added and its amount in each brine is shown in Table 1.

Table 1. Amount of salts contained in 1 L of brine.

Brine	Origin	Cations	NaCl [g]	$CaCl_2 \cdot H_2O$ [g]	$NaHCO_3$ [g]	Na_2SO_4 [g]	$MgCl_2 \cdot 6H_2O$ [g]
A	Nanofiltration	Ca^{2+}, Mg^{2+}	23.1104	1.5000	0.5000	60.0000	6.7000
B	Nanofiltration	Ca^{2+}	28.8940	1.5000	0.5000	60.0000	-
C	Reverse osmosis	Ca^{2+}, Mg^{2+}	55.4451	0.8498	0.2940	9.9996	2.5000
D	Reverse osmosis	Ca^{2+}	57.603	0.8498	0.2940	9.9996	-

These data is obtained from the previous research in the Chemical Engineering department of Universitat Politècnica de Catalunya (UPC).

Depending on the amount of calcium in each brine, which is the same for both nanofiltration (NF) brines as well as between both reverse osmosis (RO) brines, the required time to achieve the 1.67 stoichiometric molar ratio Ca/P is different. For NF brines, this time are 20 h, while for RO brines are 34.4 h.

5.3. EXPERIMENTAL PROCEDURE

To start an experiment, the reactor, must be in the correct position to assure the stirrer does not touch its walls. The 1,000 mg PO_4^{3-}/L solution can be inserted into the reactor and the mechanical mixer is connected, with a stirring speed of 250-260 rpm.

Once the pH is adjusted, a sample is taken from the reactor. The stopwatch is activated at the same time that the brine pump, that way the reactor time is measured properly.

Samples are taken from the reactor manually at different times, to have a good range of phosphate concentrations. As the experiment lasts 20 to 34 hours approximately, depending on

the type of brine, and the reaction will not be stopped during night, no samples will be taken during that period.

When the last sample is taken, the pumps and the stirring are stopped. The content of the reactor is left there to allow the bulk precipitation. After 24 hours, the reactor is emptied and cleaned, and the solution extracted is filtered using a Büchner funnel with filtering paper and a Kitasato flask thanks to a water aspirator due to Venturi effect. As soon as the solid is dry, it is weighted and kept in a plastic recipient to be later examined using different techniques such as XRD, FTIR or SEM-EDS.

5.4. ANALYTICAL METHODS

The samples taken during the experiment, which have been kept in the fridge to prevent spoilage, are analysed using spectroscopy and chromatography techniques. To do so, the samples must be diluted to have a concentration that these techniques can determine. But first they have to be filtered up to 0.2 µm. Agilent® filters are chosen since they are easy to use and provide the filtration up to 0.2 µm required for both analytical methods. On the one hand, large precipitate particles would provide erroneous absorbance values when testing the samples with spectroscopy. On the other hand, big particles would damage the chromatographer, obstructing the column.

In figure 6 pictures of the filter used (a) and the appearance of the sample before and after filtration (b) are displayed.

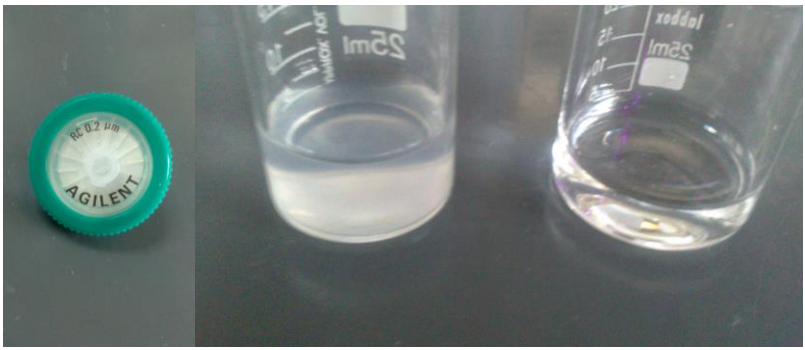

(a) (b)

Figure 6. Agilent® filter (a) and sample before and after filtration (b)

5.4.1 UV spectrophotometry

Spectrophotometry is the quantitative measurement of the reflection or transmission properties of a material as a function of wavelength. A spectrophotometer is used to measure these properties of a solution, as well as of transparent, translucent or opaque solids.

For analysing the samples taken from the reactor, Ultraviolet-visible spectrophotometry is used. This uses light in the visible and adjacent ranges.

In order to determine the concentration of substances, concretely of phosphate in the samples examined, the light transmittance of the solution can be tested using spectrophotometry. According to Beer-Lambert law, the amount of light that passes through the solution (or, the one that the solution absorbs) is indicative of the concentration of phosphate in the solution, which is the absorber.

It is necessary to know how the absorbance changes with concentration. This is determined doing a calibration curve using patterns with known concentrations. Standard solutions of 2, 5, 10 and 25 mg PO_4^{3-}/L are prepared, and then analysed with spectrophotometry. Within small ranges, Beer-Lambert law is applicable and the relationship between absorbance and concentration of absorber in the samples vary linearly. Once the calibration is done, the wavelength at which the absorbance will be tested is determined, and it is found to be 400 nm the best choice.

The absorbance at 400 nm is determined and a calibration curve is represented, absolute absorbance (calculated as absorbance at 400 nm – matrix absorbance) on the y axis and phosphate concentration on the x axis with equation y=bx+c. From this, parameters b and c are extracted, and will be used to find the concentration of phosphate when the absorbance of a sample is determined.

The methodology follows the Standard Methods. For this, a solution must be prepared with the sample to analyse and the Vanadate-Molybdate reagent. The latter will provide coloration once reacts with the phosphate contained in the sample. See Appendix 1: Preparation of solutions, to check the procedure to prepare the reagent.

Solutions are placed in a transparent cell, known as cuvette. The one used is quartz glass, and has a width of 1 cm, which is the path length, L, in the Beer-Lambert law. See figure 48 in Appendix 2: Analytical methods.

The solutions are analysed in increasing order of phosphate concentration to avoid distorted values when reusing the cuvette.

5.4.2. Ion-exchange chromatography. (Analysis of phosphate, calcium, magnesium, sodium, sulphate and chloride)

Chromatography includes various laboratory techniques which may have preparative or analytical purposes. The preparative ones separate different substances present in the sample, while the analytical purpose is to determinate qualitatively and quantitatively the substances present in the sample. In this research the main purpose is to analyse using **ion exchange chromatography** (or **ion chromatography**) the samples taken from the reactor to determine the ions present and their concentration in the samples.

The sample is the liquid analysed. It contains the substances which are going to be separated, called analytes. The stationary phase in the chromatographer used is the solid contained in the column. The mobile phase is the liquid formed by the eluent and the sample. This liquid moves through the chromatography column (stationary phase) where the sample interacts with the stationary phase and is separated. In ion-exchange chromatography, the separation takes place due to coulombic (ionic) interactions.

This type of chromatography is further subdivided into cation exchange chromatography and anion exchange chromatography. The stationary phase surface displays ionic functional groups that interact with analyte ions of opposite charge.

Cation exchange chromatography retains positively charged cations because the stationary phase contains a negatively charged functional group. The cation exchange column used is the IonPac® CS16 and the used eluent is methanesulfonic acid (MSA). It operates at 40ºC.

Anion exchange chromatography retains anions using a positively charged functional group. The anion exchange column used is the IonPac® AS23 and the used eluent is a buffer solution made of Na_2CO_3 and $NaHCO_3$. It operates at 30ºC.

The chromatogram is the visual output of the chromatograph. It is displayed on the screen of the computer which is connected to the chromatograph. Thanks to *Chromeleon* pc program, the sequence can be introduced and the results extracted once the analysis has been finished. The sequence permits the program to know how many time must the analysis of each sample last, how many samples are going to be analysed and what name they are given. A peak is a

visual representation displayed on the chromatogram that represents each of the different separated substances and its amount.

Before analysing the samples, a series of patterns containing the substances which are going to be quantified should be prepared. This allows the chromatographer to be able to identify the amount of ions presents in the sample once the peak is known, as it will be proportional to the peak formed by the known patterns.

The ion exchange chromatographer used is Thermo scientific Dionex ICS-1100 and ICS-1000, which are the anionic and cationic equipment, respectively. The automated sampler is an AS40, which automatically injects a needle into the sample container and repeats the process for all the samples to analyse.

The characteristics of the ion exchange chromatographer are summarised in table 2.

Table 2. Ion chromatography characteristics.

IonPac®	**CS16**			**AS23**		
Type	Cationic column			Anionic column		
Retains	Cations			Anions		
Ions retained	Na^+	Mg^{2+}	Ca^{2+}	PO_4^{3-}	Cl^-	SO_4^{2-}
Retention time [min]	7.24	16.77	23.49	18.81	7.22	20.62
Resin charge	Methanesulphonic Acid (MSA). Negative			Buffer solution: Na_2CO_3-$NaHCO_3$. Positive		
Operation temperature	40 ºC			30 ºC		

This ion exchange chromatographer can detect only samples with concentrations up to 300 mg/L. For this reason, the samples should be previously diluted with distilled water to a dilution factor of 100. This should be taken into account when interpreting the results obtained.

5.5. SOLID CHARACTERISATION METHODS

The solid is analysed using different techniques that provide information about its composition and crystallinity.

XRD or X-ray crystallography is a technique which determines the X-ray diffraction pattern of a crystal, and thanks to it, its molecular and atomic structure can be described. For example, in this particular case, this technique would identify crystalline hydroxyapatite in the solid obtained if it were present. X-rays are applied to the sample with a known angle while it rotates. The electrons in the atoms of the crystal scatter those rays in different directions, in what is known as elastic scattering, therefore a regular array of electrons form a multitude of waves. Destructive interferences make some waves cancel each other, while constructive interferences, which take place only when Bragg's Law is accomplished, cause a diffraction pattern.

Infrared spectroscopy analysis is the spectroscopy that uses the infrared region of the electromagnetic spectrum to generate IR spectra. When a compound is radiated with a frequency that matches perfectly with the frequency of one of its vibrations, the molecule absorbs energy. Absorption bands of the different functional groups constituting the molecule studied appear at different frequencies (position), with different intensities (weak, medium or strong) and shape (broad or sharp). Thanks to these characteristics, the molecule can be identified. Fourier Transform Infrared Spectrometer (**FTIR**) radiates the sample with a beam containing many frequencies of light at the same time, and measures the amount of it absorbed by the sample.

FESEM (Field Emission Scanning Electron Microscope) produces images of a sample when scanning it with a beam of electrons. The atoms in the sample interact physically with the light beam and an image can be created with the signal received by the bouncing of the surface irregularities. This provides a picture of the superficial texture. It also allows determining the percentage of each substance in the superficial layer of the solid.

To prepare the samples that are later introduced into the microscope, the solids have to be heated in the oven for 24 h. Then they are placed on a metal support which is coated by a carbon sticker. This attracts the electron beam to the samples, allowing a high resolution vision. But to ensure a complete conductivity of the material analysed, the sample is coated with a platinum-palladium mixture. To do this, the plaque is introduced in the Cressington Sputter

Coater 208 HR (see figure 65 and 66 in Appendix 2: Analytical methods), the void is done and an argon blanketing takes place. On one pole there is a platinum-palladium piece of metal and a voltage difference is applied. This causes this platinum and palladium ions to migrate from one pole to the other pole. In their way, the sample is impeding this movement, causing it to be coated by the two metals. The duration of this process determines the thickness of the metal coat, which is at least 22 nm thick.

The Field Emission Scanning Electron Microscope used is JEOL JSM-7001F (see figure 67 in Appendix 2: Analytical methods), and the computer program used to operate it is INCA. By this technique magnifications up to x 100,000 can be achieved. The microscope has two chambers. The first one, which is in contact with the exterior, acts as a pressure regulator. The pressure in the interior of the second chamber, where the sample is moved once the opening is sealed is $6.5 \cdot 10^{-4}$ Pa. The vacuum should be constant to take the best pictures and to avoid distortion.

Other techniques to analyse solids are the following:

BET (Brunauer–Emmett–Teller) theory is the basis for the analyse technique that measures the specific surface area of a material. Furthermore, this is a way to determine the texture of the solid obtained.

Dynamic Laser Scattering (DLS) is used to characterize size of various particles including proteins, polymers, micelles, carbohydrates, and nanoparticles. With this, the diameter of the hydroxyapatite nanoparticles can be determined.

Differential Scanning Calorimetry (DSC) is widely used to determine the purity of the solid, being related with its fusion point, which can be easily determined.

6. RESULTS AND DISCUSSION

Here the results obtained from the experiments will be shown. The phosphate removal and the effect of different parameters on it will be discussed. The analysis of the solids obtained by means of XRD, FTIR and SEM methods will be used to corroborate the hypothesis raised. Finally a comparison of the experiments will take place, enabling the drawing of the conclusions.

6.1. PHOSPHATE PRECIPITATION USING NANOFILTRATION AND REVERSE OSMOSIS BRINES

Each experiment tests a unique combination of parameters to observe the differences present. The first four tests take place at pH=10.5, while the last four repeat the same conditions at pH=12. Experiments are named using either their description or their number, as summarised in table 3.

Table 3. Experiment characteristics.

EXPERIMENT	Section	Brine	Ca^{2+} and Mg^{2+} origin	pH
1	6.1.1.	A	NF (Ca^{2+}, Mg^{2+})	10.5
2	6.1.2.	B	NF (Ca^{2+})	10.5
3	6.1.3.	D	RO (Ca^{2+})	10.5
4	6.1.4.	C	RO (Ca^{2+}, Mg^{2+})	10.5
5	6.1.5.	A	NF (Ca^{2+}, Mg^{2+})	12
6	6.1.6.	B	NF (Ca^{2+})	12
7	6.1.7.	D	RO (Ca^{2+})	12
8	6.1.8.	C	RO (Ca^{2+}, Mg^{2+})	12

6.1.1. Experiment 1. Nanofiltration brine (with Mg^{2+}) at pH=10.5

This experiment is carried out using nanofiltration brine with magnesium (brine A) at pH=10.5. In figure 7 it is shown the phosphate concentration, in ppm, or mg PO_4^{3-}/L with time. A significant decrease can be appreciated, as phosphate precipitates. The values represented are the arithmetic mean between the values obtained using spectrophotometry and chromatography methods.

The phosphate removal is 96.84%. This reflects the effectiveness of the removal in the conditions of pH=10.5 and presence of magnesium in a simulated nanofiltration brine.

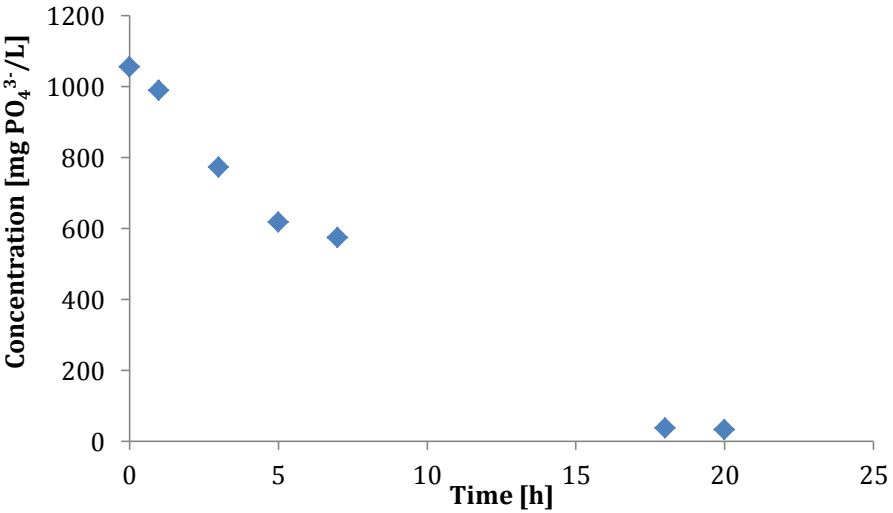

Figure 7. Phosphate concentration with time. Exp. 1. Nanofiltration brine (with Mg^{2+}) at pH=10.5.

In figure 8, the concentration of the other ions is shown. The growing amount of sulphate, sodium and chloride responds to the introduction of the brine solution into the reactor. In these three there is a decrease between the two last samples, which correspond to the formation of a precipitate at 18 h after the start of the experiment.

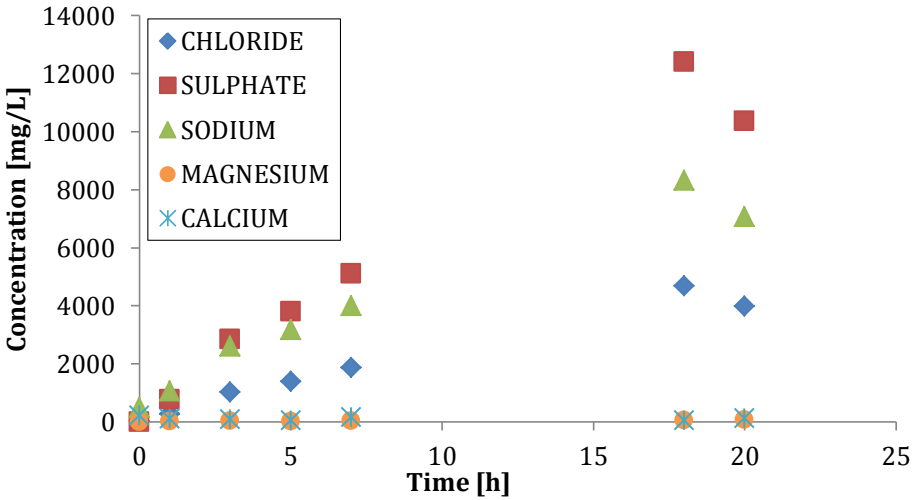

Figure 8. Concentration of the different ions with time. Exp. 1. Nanofiltration brine (with Mg^{2+}) at pH=10.5.

Precipitation has been taking place during all the experiment as figures 9 to 11 reflect. Without reaction of precipitation, the concentration in the reactor would be much bigger, as drawn with the grey line. Sodium concentration is much smaller than the expected without reaction and this difference is more marked than in sulphate and this in term more than chloride. This points out that the sodium precipitation is bigger than the sulphate and the chloride ones. Note the different scale of figures 9 to 11, as it can be visually misinterpreted.

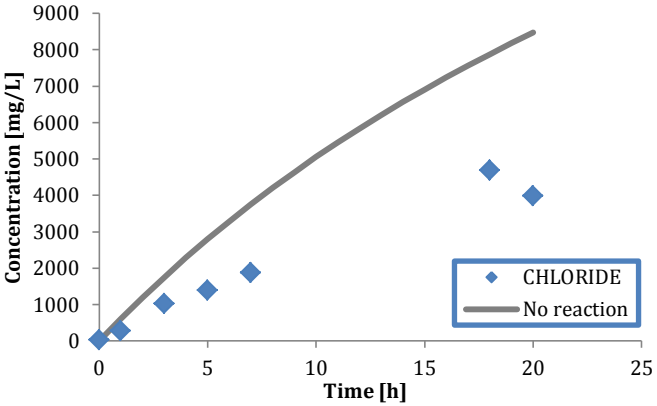

Figure 9. Chloride concentration with time. Exp. 1. Nanofiltration brine (with Mg^{2+}) at pH=10.5

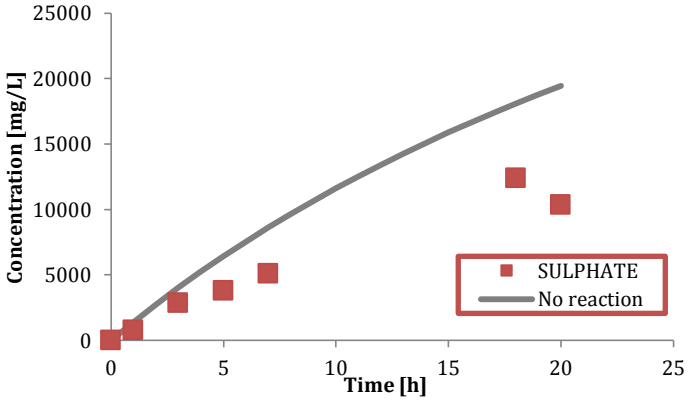

Figure 10. Sulphate concentration with time. Exp. 1. Nanofiltration brine (with Mg^{2+}) at pH=10.5.

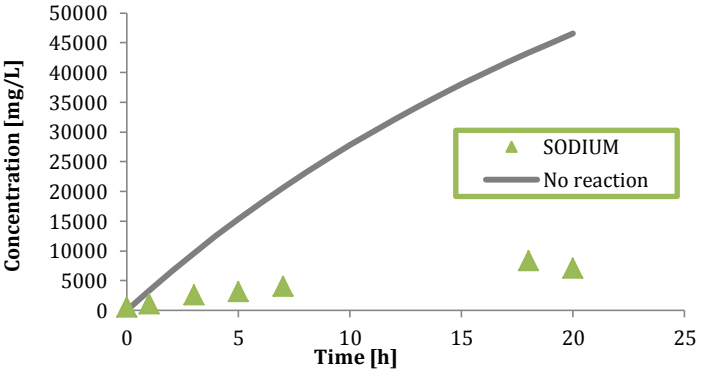

Figure 11. Sodium concentration with time. Exp. 1. Nanofiltration brine (with Mg^{2+}) at pH=10.5.

In figure 12 magnesium concentration in the solution is illustrated, a slight growth can be observed due to the accumulation of it in the reactor. Precipitation of a magnesium salt is taking place, as these concentrations are smaller than the ones if there was no reaction.

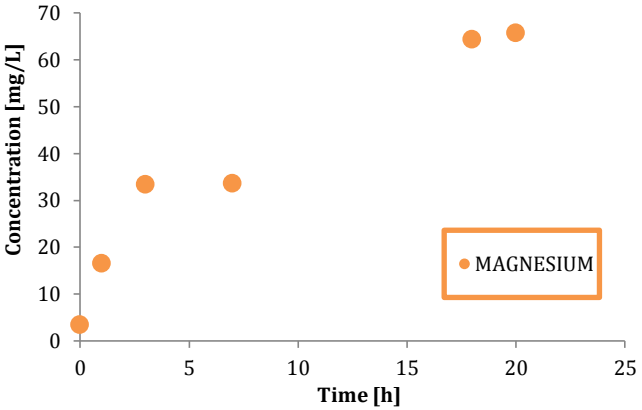

Figure 12. Calcium and magnesium concentration with time. Exp. 1. Nanofiltration brine (with Mg^{2+}) at pH=10.5.

As will be seen in the coming observations, this magnesium arise also appears in experiment 4, where similar conditions are applied in the presence of magnesium.

6.1.2. Experiment 2. Nanofiltration brine at pH=10.5

This experiment is carried out using nanofiltration brine without magnesium (brine B) at pH=10.5.

The concentration slope is much more flat than in the previous experiment. The nucleation time is longer as seen in figure 13.

The phosphate removal is 41.76%. This conditions of pH=10.5 without magnesium in simulated nanofiltration brine remove much less phosphate than the previous one.

In figure 14 the evolution is very similar to the one seen in experiment 1, but now there is no decrease in the final hours of experiment. The concentration stabilises achieving a value.

As in the previous experiment, the comparison between the expected concentration if it were no precipitation reaction and the analysis results demonstrates the precipitation of chloride, sulphate and sodium salts.

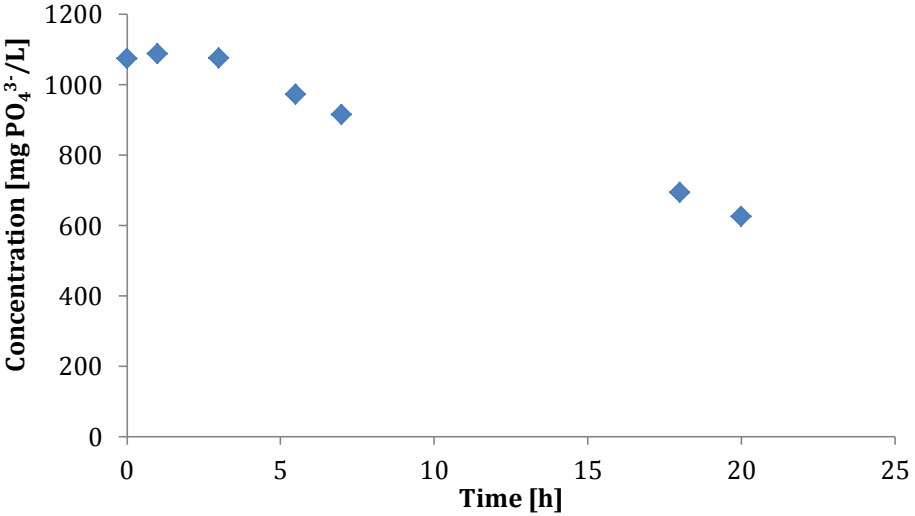

Figure 13. Phosphate concentration with time. Exp. 2. Nanofiltration brine at pH=10.5.

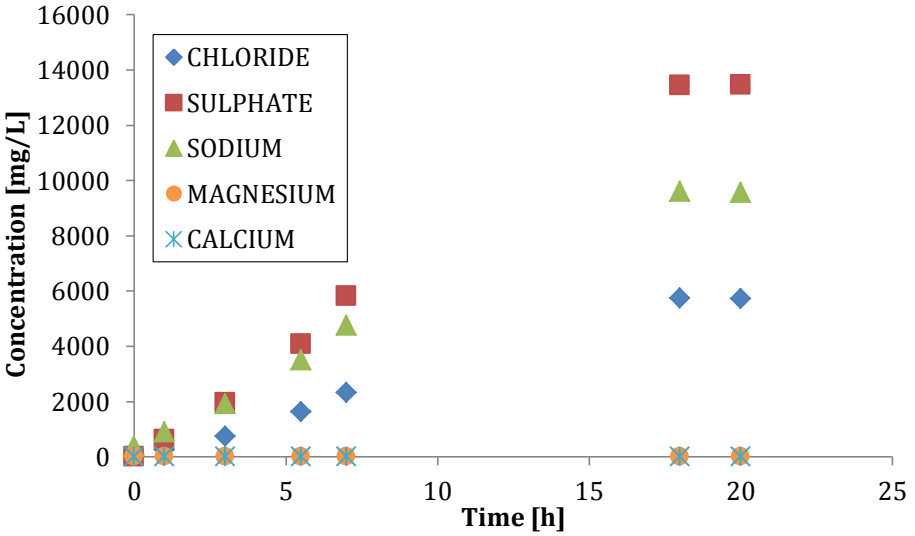

Figure 14. Concentration of the different ions with time. Exp. 2. Nanofiltration brine at pH=10.5.

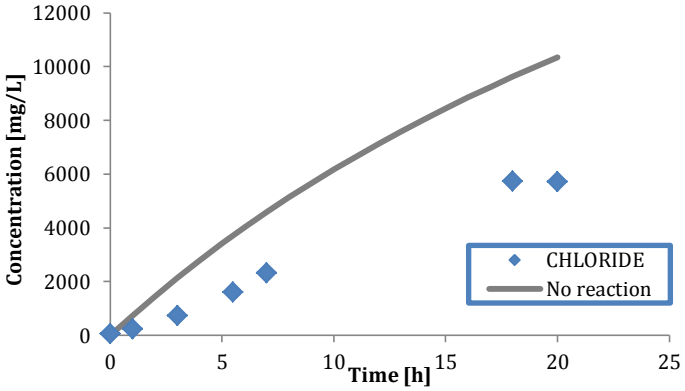

Figure 15. Chloride concentration with time. Exp. 2. Nanofiltration brine at pH=10.5.

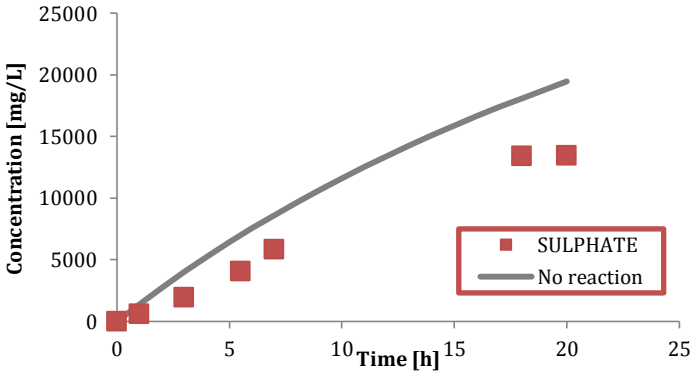

Figure 16. Sulphate concentration with time. Exp. 2. Nanofiltration brine at pH=10.5.

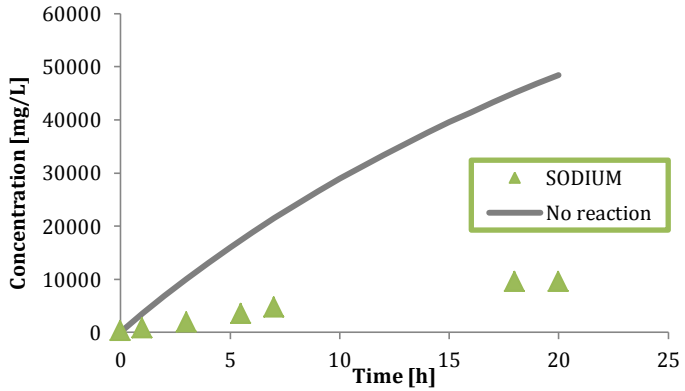

Figure 17. Sodium concentration with time. Exp. 2. Nanofiltration brine at pH=10.5.

As in experiment 1, the chloride is the one that less precipitates, as it is not so far away from its non-reaction curve (figure 16). Sodium and chloride precipitate, and possibly in halite form (NaCl). That would explain the large amount of these ions removed from the solution (figures 15 and 17).

In this experiment no magnesium or calcium is detected by ion chromatography. The lack of magnesium in the brine used is corroborated with these results. Apparently, calcium precipitates once it enters the reactor and therefore there is no presence of it in the solution.

6.1.3. Experiment 3. Reverse osmosis brine at pH=10.5

This experiment is carried out using reverse osmosis brine without magnesium (brine D) at pH=10.5. Phosphate concentration is exposed in figure 18.

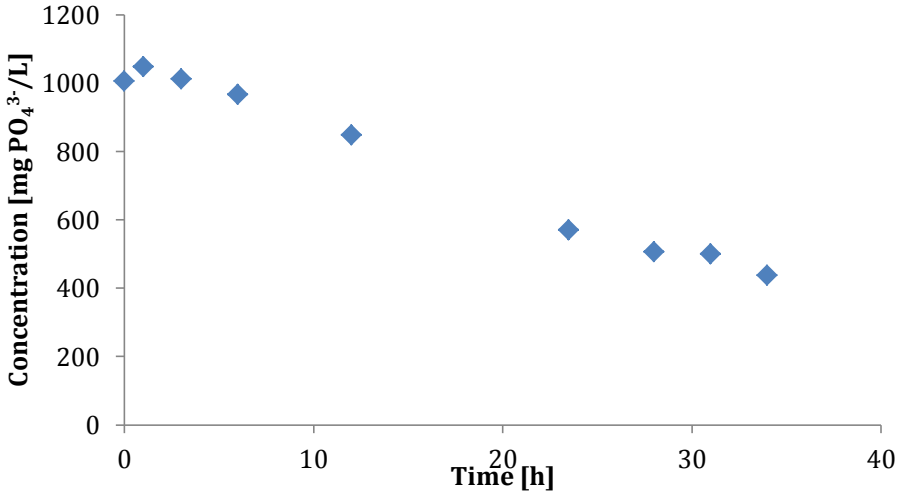

Figure 18. Phosphate concentration with time. Exp. 3. Reverse osmosis brine at pH=10.5.

The phosphate removal is 56.47%. As in the previous experiment, these conditions of pH=10.5 without magnesium in a simulated reverse osmosis brine do not remove as much phosphorus as in experiment 1, when Mg^{2+} was present. This concentration decrease is one of the softer, and the nucleation period is not sharply drawn, meaning it takes longer and the crystal growth is slow.

As a result to the brine type change in this reaction, the amount of the different ions has inverted (figure 19). Reverse osmosis brine contains fewer grams of sodium sulphate than

nanofiltration, which is the salt that provides the brine with SO_4^{2-}. At the end, there is another precipitation involving chloride and sodium, which could be halite.

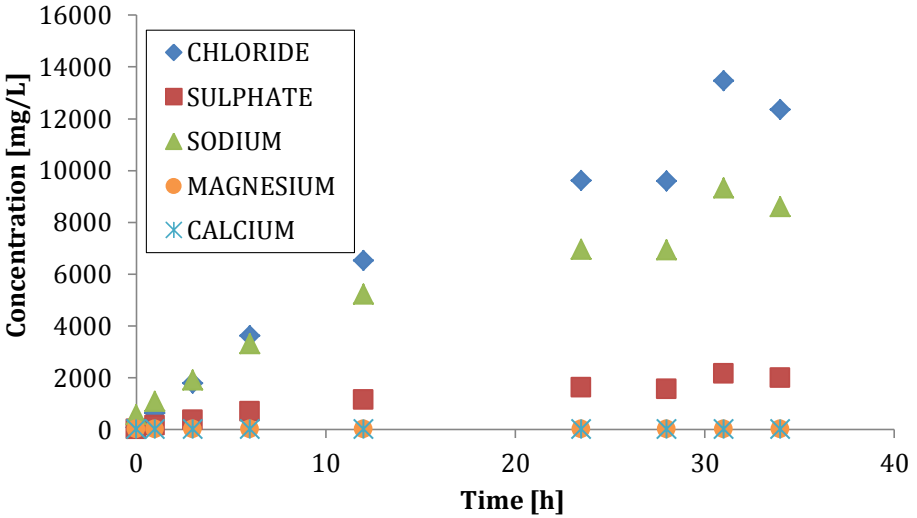

Figure 19. Concentration of the different ions with time. Exp. 3. Reverse osmosis brine at pH=10.5.

As in experiment 2, here no magnesium or calcium is detected by ion chromatography, due to the lack of Mg^{2+} in the brine and the immediate precipitation of Ca^{2+} when in contact with the phosphate solution.

6.1.4. Experiment 4. Reverse osmosis brine (with Mg^{2+}) at pH=10.5

This is the last experiment at pH=10.5. Reverse osmosis brine with magnesium (brine C) is used. As can be observed in figure 20, there is a short constant period followed by a steep decrease of the phosphate concentration. This is a result of magnesium presence. The initial phosphate concentration was not 1,000 ppm, the ideal to obtain HAP in 20 h, but the phosphate removal was very satisfactory.

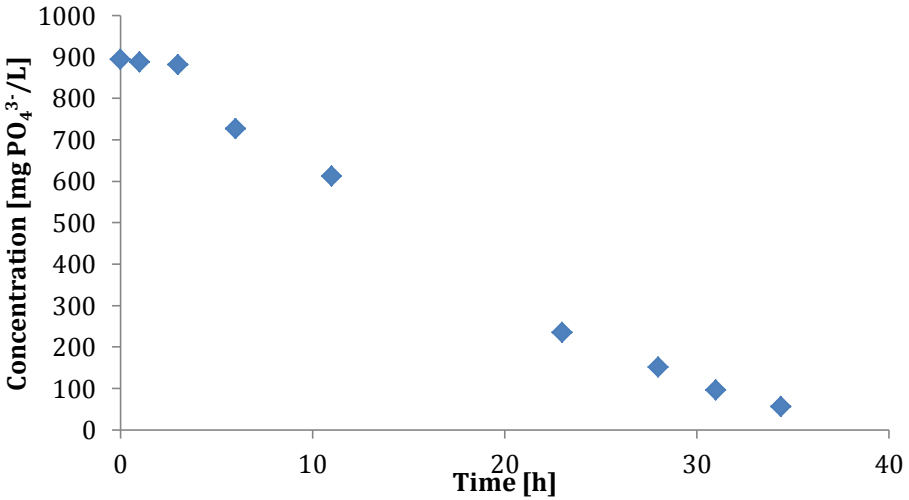

Figure 20. Phosphate concentration with time. Exp. 4. Reverse osmosis brine (with Mg^{2+}) at pH=10.5.

The nucleation period is shorter, and the growth is faster as proved by the rapid drop. The phosphate removal is 93.66%. Much more removal is accomplished, as in the first experiment, which also had Mg^{2+}.

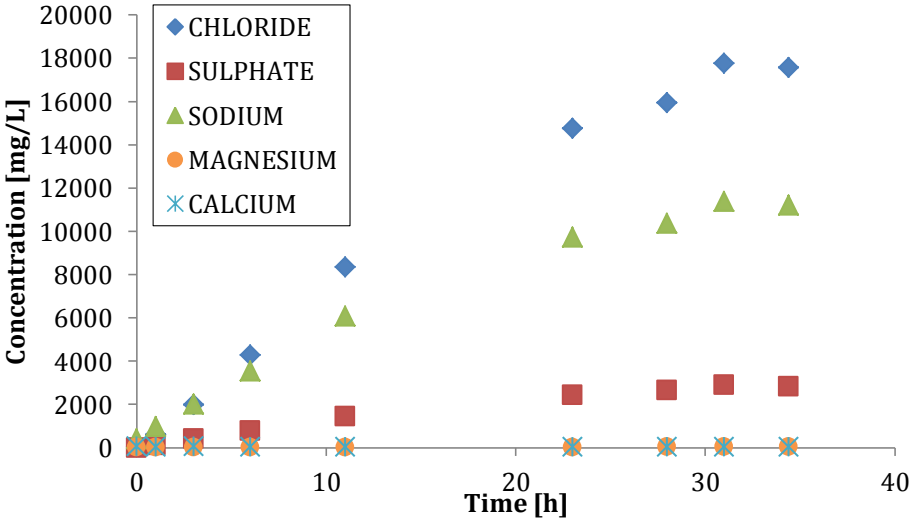

Figure 21. Concentration of the different ions with time. Exp. 4. Reverse osmosis brine (with Mg^{2+}) at pH=10.5.

Mg^{2+}, added to the reactor with the brine, describe an increment in concentration (Figure 22) but is far away from the theoretical concentration if no reaction occurred. This confirms the Mg^{2+} precipitation.

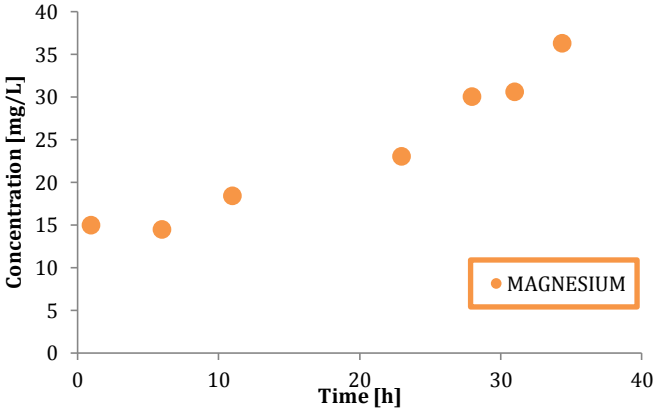

Figure 22. Mg^{2+} concentration with time. Exp. 4. Reverse osmosis brine (with Mg^{2+}) at pH=10.5.

6.1.5. Experiment 5. Nanofiltration brine (with Mg^{2+}) at pH=12

From this experiment on, the first four tests are repeated at pH=12.

Nanofiltration brine with magnesium is used and a much more lineal decrease is observed in figure 23. There is almost no nucleation plain, which suggests that the precipitate growth is faster. The remaining phosphate concentration is about 140 mg PO_4^{3-}/L, which represents 86% of removal.

Although the used NF brine incorporates Mg^{2+}, it precipitates and does not remain in the solution, as does Ca^{2+}.

Heterogeneous precipitation is found in the wall of the reactor. Foreign surfaces enhance the nucleation process.

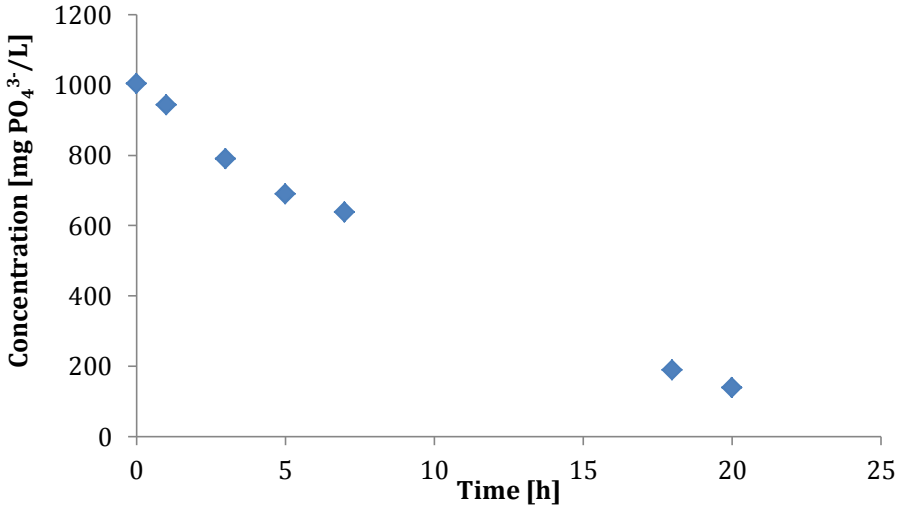

Figure 23. Phosphate concentration with time. Exp. 5. Nanofiltration brine (with Mg^{2+}) at pH=12.

Cl^-, SO_4^{2-} and Na^+ describe a similar increase to figure 25, as both experiments share the same type of brine.

6.1.6. Experiment 6. Nanofiltration brine at pH=12

Nanofiltration brine without magnesium at pH=12. The phosphate removal is slow and inefficient. Not even a 40% of removal is achieved, so these are not good conditions for this goal. Figure 24 presents analytical results, where, as in experiment 2 (same conditions at pH=10.5), long nucleation time is required and poor efficiency is achieved.

Neither calcium nor magnesium (as expected due to the lack of Mg^{2+} in the brine) were found on the solution.

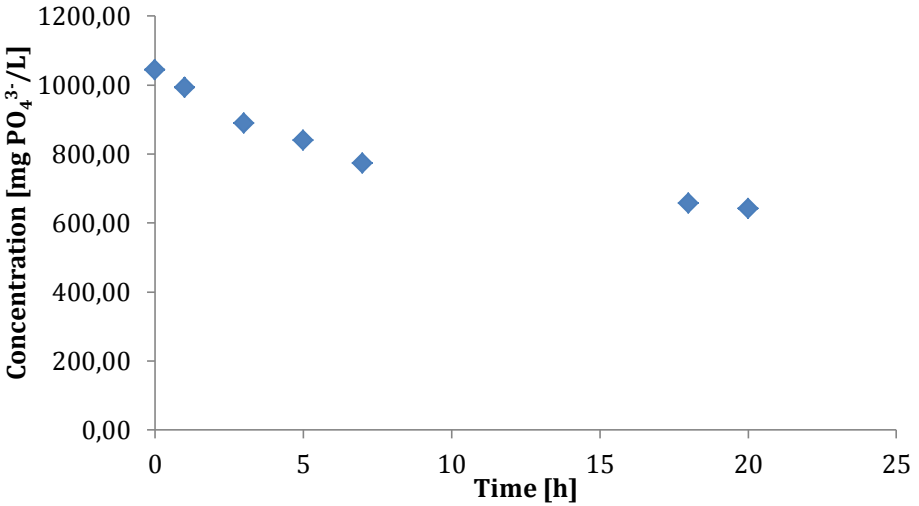

Figure 24. Phosphate concentration with time. Exp. 6. Nanofiltration brine at pH=12.

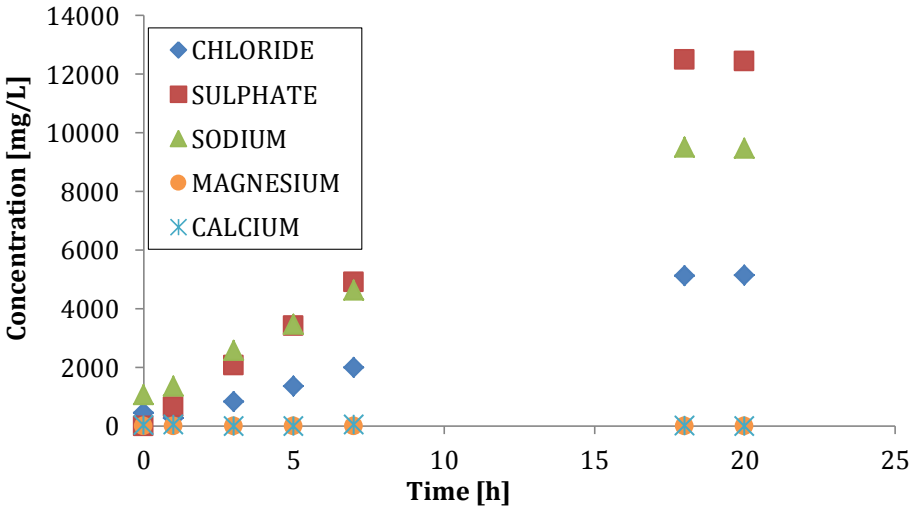

Figure 25. Concentration of the different ions with time. Exp. 6. Nanofiltration brine at pH=12.

NF brine experiments are shorter and, due to the limitations of the experimental procedure, have a large period of time without samples taken. With further research, more points could be determined by changing the starting hour so that extractions at 10-15 h would be during the day.

6.1.7. Experiment 7. Reverse osmosis brine at pH=12

Reverse osmosis brine without magnesium at pH=12. 51.75% phosphate removal is obtained. The nucleation period is longer and the slope is small, as in experiment 6.

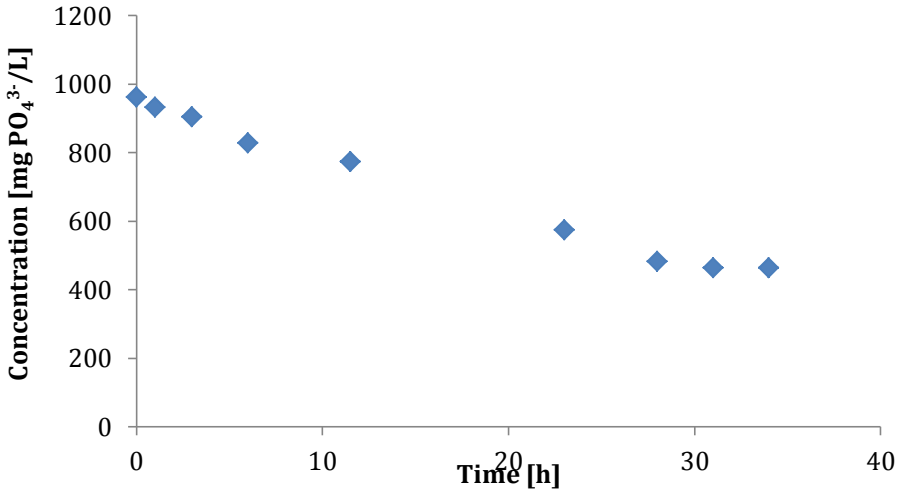

Figure 26. Phosphate concentration with time. Exp. 7. Reverse osmosis brine at pH=12.

The rest of the ions, as in the other experiments, describe a correct increase according to the brine pumped into the reactor.

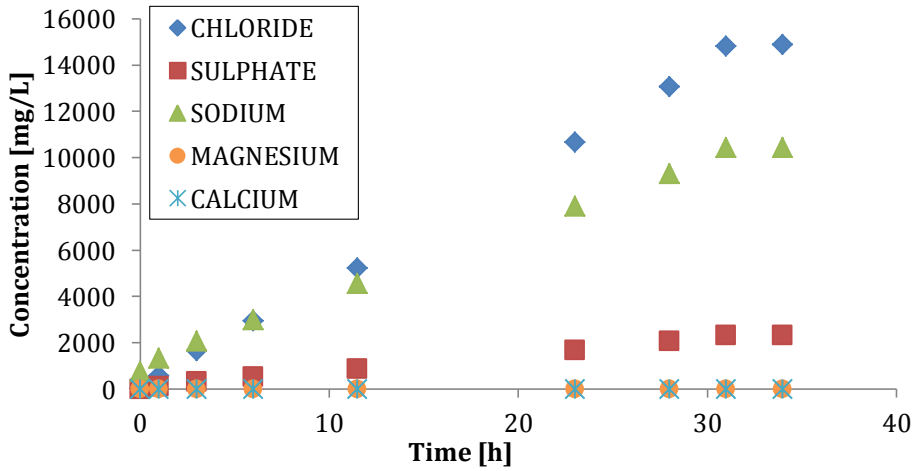

Figure 27. Concentration of the different ions with time. Exp. 7. Reverse osmosis brine at pH=12.

6.1.8. Experiment 8. Reverse osmosis brine (with Mg^{2+}) at pH=12

The last experiment performs RO brine with magnesium at pH=12. The remaining phosphate concentration in the solution was 370 mg PO_4^{3-}/L.

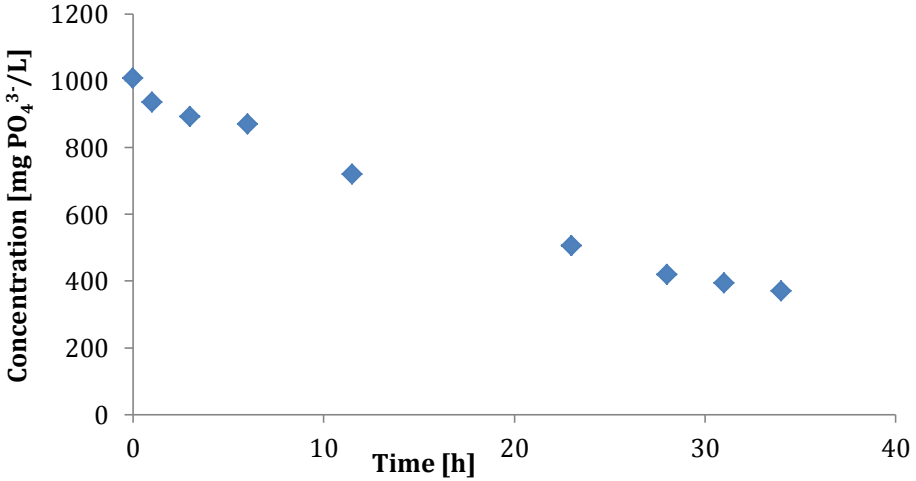

Figure 28. Phosphate concentration with time. Exp. 8. Reverse osmosis brine (with Mg^{2+}) at pH=12.

Phosphate removal efficiency is only 63.26%. Ca^{2+} and Mg^{2+} cations were not detected in the solution during the precipitation and the evolution of Cl^-, SO_4^{2-} and Na^+ ions reflect a normal increase, confirming that the pumps were operating correctly and that no interruption took place during the experiment.

6.2. SOLID CHARACTERISATION OF THE OBTAINED PRECIPITATE

Using multiple observations of a specimen increases the probability of a successful identification. In this section, the results obtained using XRD, FTIR and SEM techniques are commented. All the SEM pictures can be found in Appendix 3: Solid characterisation, as in this section only some representative ones are discussed.

6.2.1. XRD

The results of this technique are usually represented in a graphic with the intensity (counts/s) plotted on the Y-axis and 2θ on the X-axis. The latter is the angle of the detector in relation with the direction of the incident ray, as schematised in figure 29.

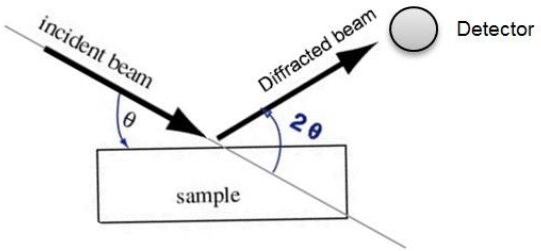

Figure 29. XRD analysis geometry.

(Image adapted from http://www.trincoll.edu/~cgeiss/GEOS_112/XRD/xrd_lab.htm)

Crystalline hydroxyapatite obtained in experiments 3 and 6, as identified in X-ray diffraction analysis (shown in red in figures 30 and 31). The highest peak of intensity appears when 2θ=32º, and another peak protrudes at 2θ=26º. There are other smaller peaks around 50º. The distribution of HAP peaks is compared to the ones in JCPDS 9–0432 file of the ICDD (International Centre for Diffraction Data) database to identify hydroxyapatite.

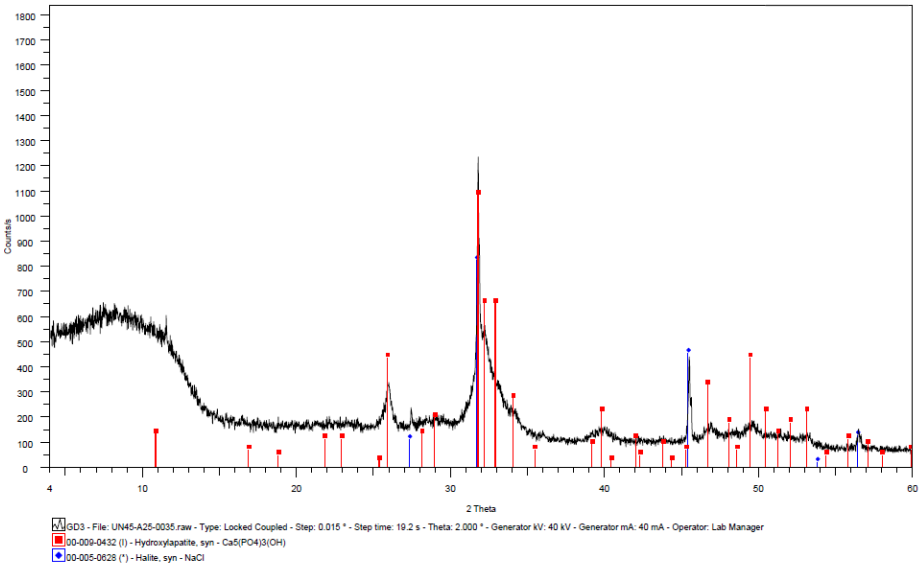

Figure 30. X-Ray diffraction analysis. Exp.3. Reverse osmosis brine at pH=10.5.

Phosphate removal in experiment 6 was slow and inefficient, but, on the contrary, HAP has been obtained.

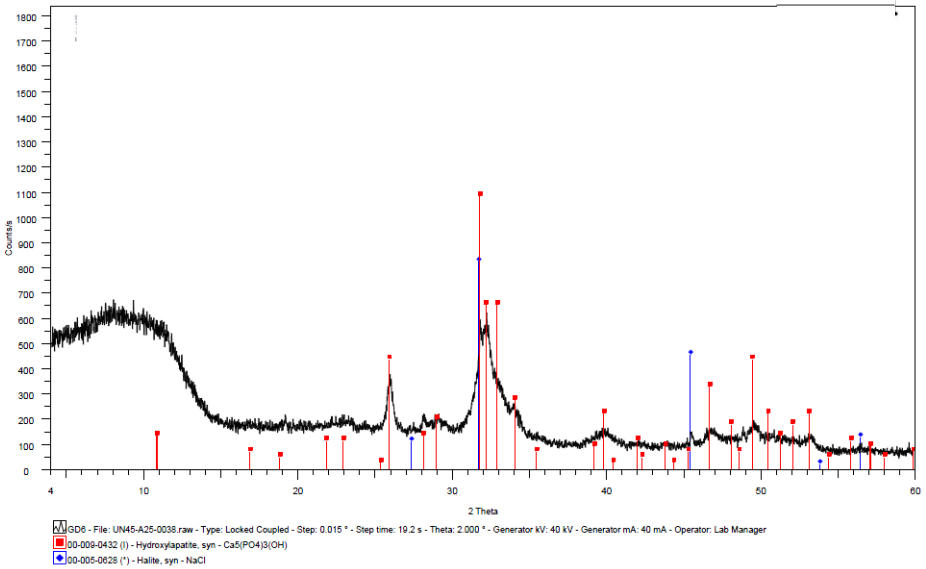

Figure 31. X-Ray diffraction analysis. Exp. 6. Nanofiltration brine at pH=12.

Some halite is also detected, shown in blue in the same figures 30 and 31.

This result corroborates the hypothesis that the chloride and sodium precipitation were in form of halite. (Section 6.1.3. Experiment 3. Reverse osmosis brine at pH=10.5).

Crystalline halite (NaCl) was found in experiment 8, RO brine (with Mg^{2+}) at pH=12. See figure 64 in Appendix 3: Solid characterisation.

6.2.2. FTIR

FTIR it is usually a complementary tool to XRD. The results of this technique are represented in a graphic with the Transmittance (%) plotted on the Y-axis and wavenumber (cm^{-1}) on the X-axis. Absorption bands observed in figures 32 and 33 confirm the idea that the solid obtained in experiments 3 and 6 is hydroxyapatite. The functional groups present in HAP are identified in both IR spectra. OH- group absorption band is broad, located at 3,388 cm^{-1} (figure 32) and 3,333 cm^{-1} (figure 33), within the 3,200-3,650 cm^{-1} interval. Phosphate is identified with different absorption bands, one for each of its chemical bonds. Especially in hydroxyapatite, the

identification of the phosphate is complex. Phosphate can be identified with the band at 960 cm^{-1} approximately (revealing P-OH bond, *v*1), which not visible because it is very close to the strongly intense 1,017 cm^{-1} band (*v*3, bending mode). There is a medium intensity band at around 500-600 cm^{-1} (*v*4, bending mode) and finally at 460 cm^{-1}, unfortunately out of the graphic, there should be the *v*2 bond, these four indicate the phosphate presence. The weak intensity band at 1,650 cm^{-1} (seen in both figure 32 and 33) due to bending vibrations, point out the strongly absorbed water.

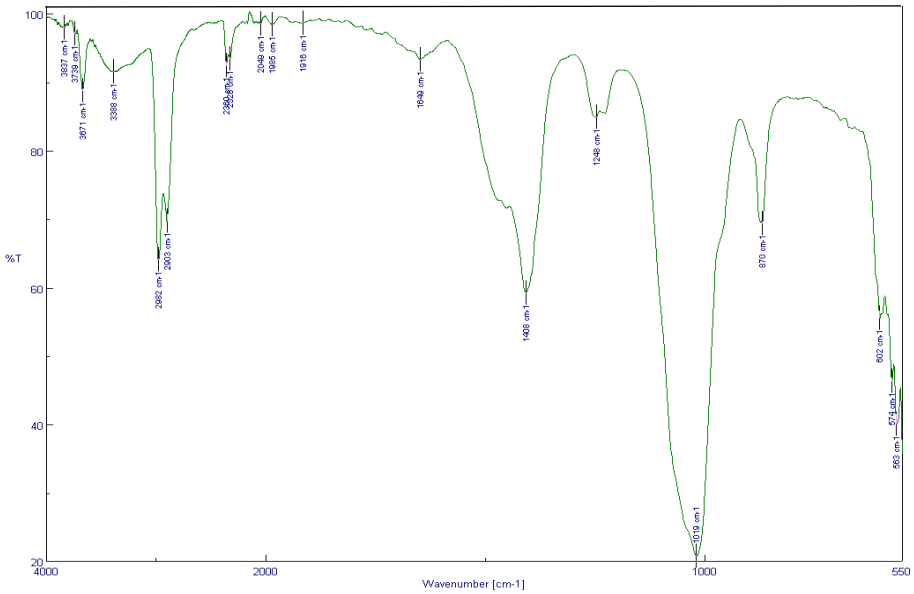

Figure 32. IR spectrum. Exp. 3. Reverse osmosis brine at pH=10.5.

Calcium deficient HAP is identified by a band at 875 cm^{-1} (Raynaud et al., 2002). In figures 32 and 33 a similar band at 870 cm^{-1} and 878 cm^{-1}, respectively is found.

Hydroxyapatite has been detected using XRD methodology and IR spectroscopy verifies it.

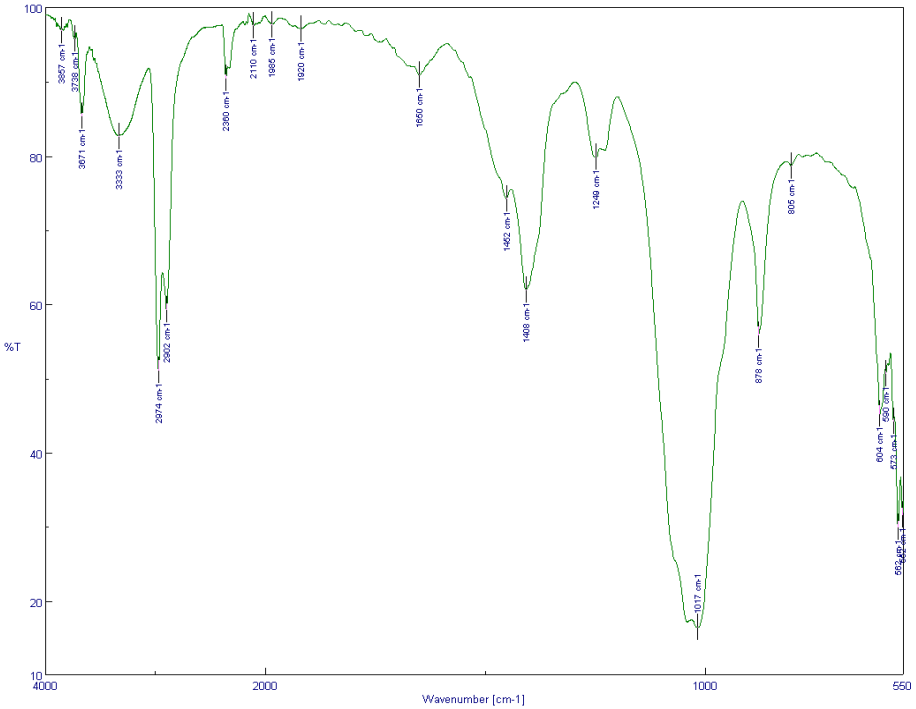

Figure 33. IR spectrum. Exp. 6. Nanofiltration brine at pH=12.

6.2.3. SEM

SEM micrographs at different magnifications were taken from the solids obtained. Samples containing hydroxyapatite are shown in figures 34 and 35. The rest of the micrographs can be found in Appendix 3: Solid characterisation.

Figure 34 is the SEM micrograph of the precipitate using RO brine without Mg^{2+} at pH=10.5 (exp. 3). High dispersion in particle size is detected, as size range is 1-10 μm approximately. Figure 57 in Appendix 3: Solid characterisation shows spherical particles of the solid obtained (x 50,000 magnifications).

Crystals created in experiment 6 have a more homogeneous area (figure 35), with a particle size range of 3-10 μm approximately.

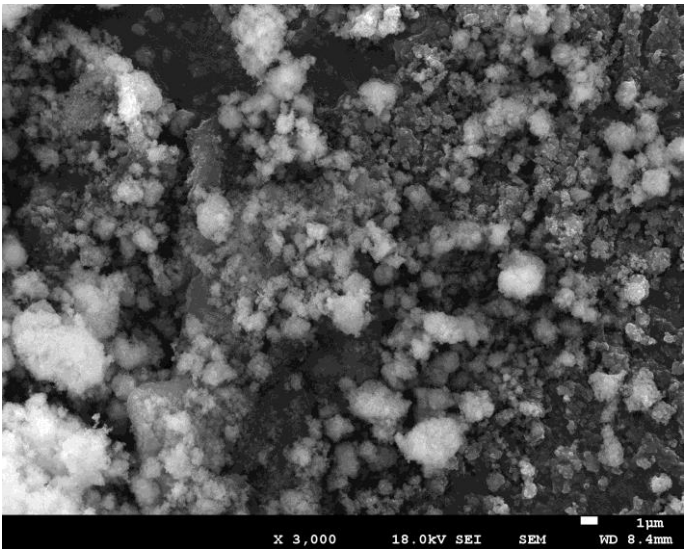

Figure 34. SEM micrograph (x 3,000 magnifications). Exp. 3. Reverse osmosis brine at pH=10.5.

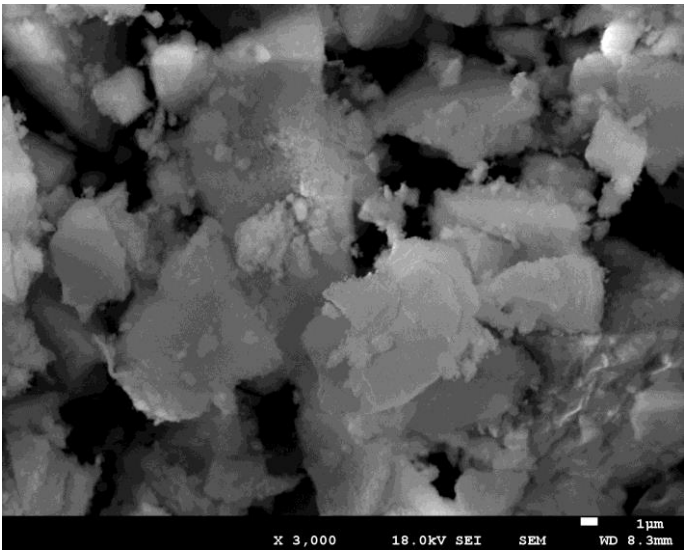

Figure 35. SEM micrograph (x 3,000 magnifications). Exp. 6. Nanofiltration brine at pH=12.

With Energy Dispersion Spectroscopy (EDS), a determination of the chemical species present in the surface of the sample can be done. Counts per second (cps) are plotted on the Y-axis and keV on the X-axis to create a spectrum diagram.

In figure 37, the calcium-phosphate-oxygen relation is coherent with the hydroxyapatite, as calcium is more abundant than phosphate and this in turn higher than oxygen.

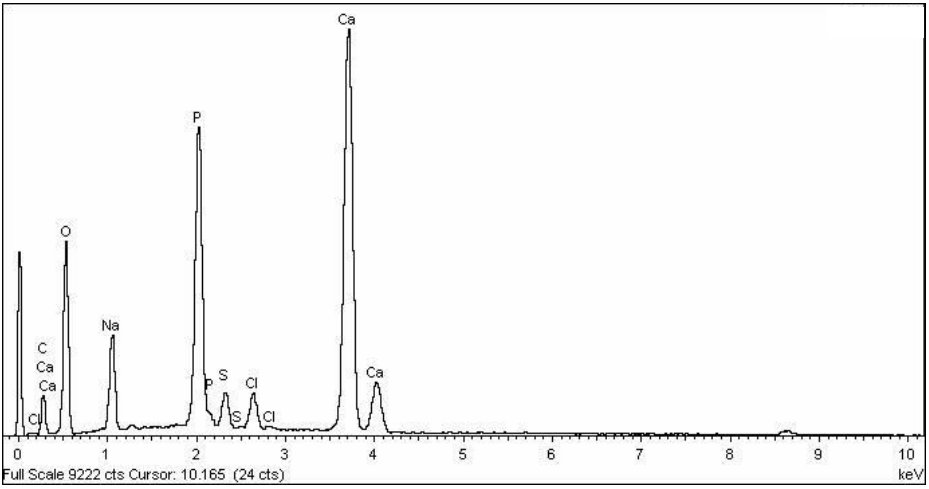

Figure 36. EDS spectrum. Exp. 6. Nanofiltration brine at pH=12.

The spectrum obtained in experiment 6 corroborates the results obtained by XRD and IR methods that the solid obtained in experiment 6 is hydroxyapatite. Figure 37 shows a close-up of the obtained HAP (x 50,000 magnifications).

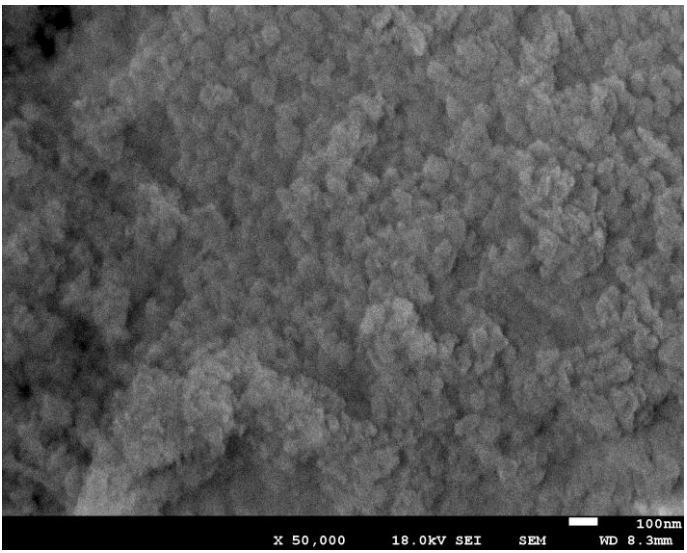

Figure 37. SEM micrograph (x 50,000 magnifications). Exp. 6. Nanofiltration brine at pH=12.

EDS semi-quantitative determination of the elemental composition in the surface of the solids obtained confirms the presence of Cl, S, O, C, Na, P and Ca in all the solids. Mg only detected in experiments 1, 4, 5 and 8, supporting the idea of the precipitation of the ions added with the brine, and justifying the difference between the concentration in the solution if it were no reaction and the experimental concentrations in the extracted samples.

6.3. COMPARATIVE STUDY OF THE RESULTS OBTAINED

The experiments on its own do not give an idea of the effect of the different parameters that have been changed. By comparing them, it is easier to select the best conditions according to the established objectives. Table 4 summarises the characteristics of each experiment and the results obtained.

Table 4. Summary of experimental results of the phosphate precipitation with NF and RO brines.

EXPERIMENT	Ca^{2+} and Mg^{2+} origin	pH	Phosphate removal [%]	Solid obtained [g]	Crystallinity of solids
1	NF (Ca^{2+}, Mg^{2+})	10.5	96.84	1.409	Amorphous
2	NF (Ca^{2+})	10.5	41.76	0.845	Amorphous
3	RO (Ca^{2+})	10.5	56.47	0.941	Crystalline HAP
4	RO (Ca^{2+}, Mg^{2+})	10.5	93.66	1.319	Amorphous
5	NF (Ca^{2+}, Mg^{2+})	12	86.10	2.291	Amorphous
6	NF (Ca^{2+})	12	38.56	0.636	Crystalline HAP
7	RO (Ca^{2+})	12	51.75	0.885	Amorphous
8	RO (Ca^{2+}, Mg^{2+})	12	63.26	2.145	Crystalline halite

X-ray diffraction found amorphous solids and, therefore, could not identify crystalline forms of calcium phosphate or other phosphate forms in some samples. Using other techniques, better determinations can be done and the % of the different salts found.

6.3.1. Effect of Mg^{2+}

In this section the effect of magnesium will be discussed, as it has been proved that affects to both phosphate removal and the obtained precipitate.

6.3.1.1. On the phosphate removal

When Mg^{2+} is present, the removal % is bigger. The amount of phosphate that remains in the reactor is in average 150.11 mg PO_4^{3-}/L when Mg^{2+} is present, which is an 84.96 % of removal. On the other case, when this cation is not present, the average removal is only up to 47.13 %, leaving the remaining solution with 542.43 mg PO_4^{3-}/L. This leads to the conclusion that the presence of Mg^{2+} in the brine solution increases the amount of phosphate removed by precipitation (figure 38).

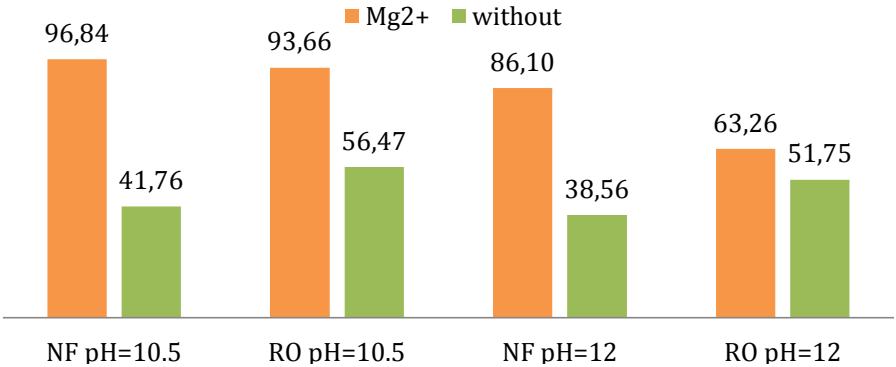

Figure 38. Effect of Mg^{2+} on the phosphate removal.

Another tendency that can be observed is the fact that the phosphate concentration curve with time is different whether there is Mg^{2+} or not. If there is, the decreasing slope is more abrupt and the nucleation period is shorter. Then there is a lack of Mg^{2+}, the slope is softer and the nucleation time seems to take longer, as shown in figure 39.

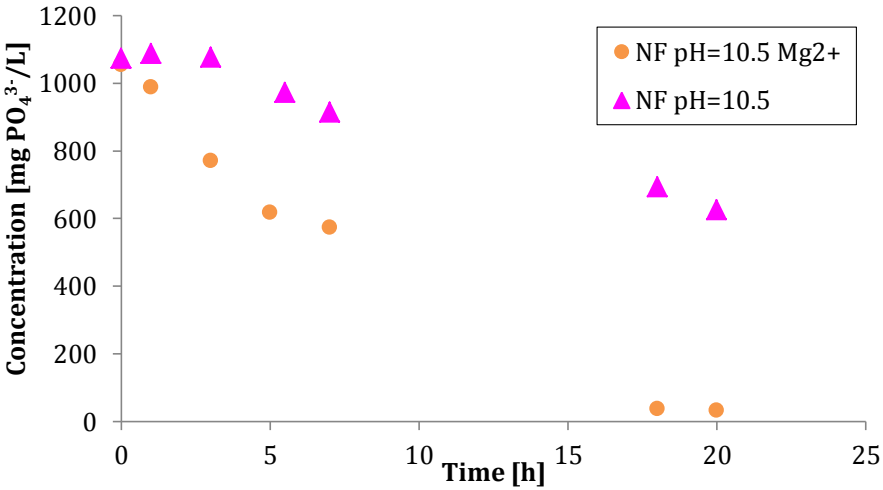

Figure 39. Phosphate concentration slope comparative.

6.3.1.2. On the solid obtained

On the solid obtained, the effect of Mg^{2+} is important: it increases the amount of solid precipitated, as figure 40 corroborates. As HAP was not found in the experiments containing Mg^{2+}, this cation impedes the formation on this type of calcium phosphate.

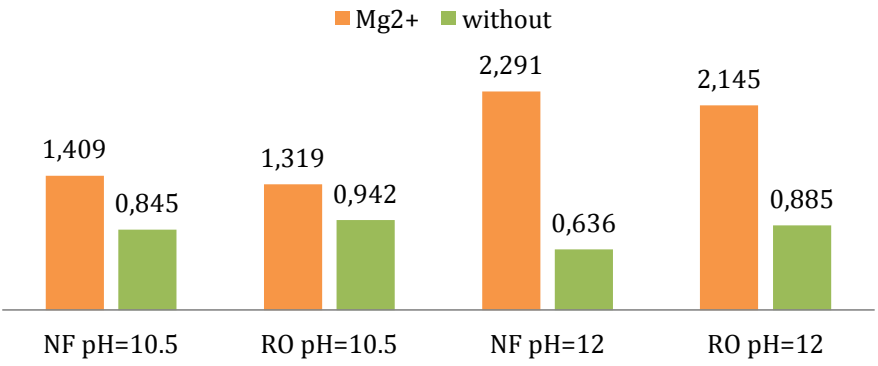

Figure 40. Effect of Mg^{2+} on the amount of solid obtained.

6.3.2. Effect of pH

The alkalinity of the solution is important as is affects directly to the behaviour of the different species in the system studied.

6.3.2.1. On the phosphate removal

Figure 41 compares the phosphate removal efficiency of all the experiments. In all cases, higher removal is achieved at pH=10.5, although with little difference in general. But when using reverse osmosis brines with Mg^{2+}, the distinction is enough to affirm that this level of alkalinity is better. If the objective is to remove the phosphate, the NF and RO brines with Mg^{2+} at pH=10.5 are the best options, having almost a 100% of removal.

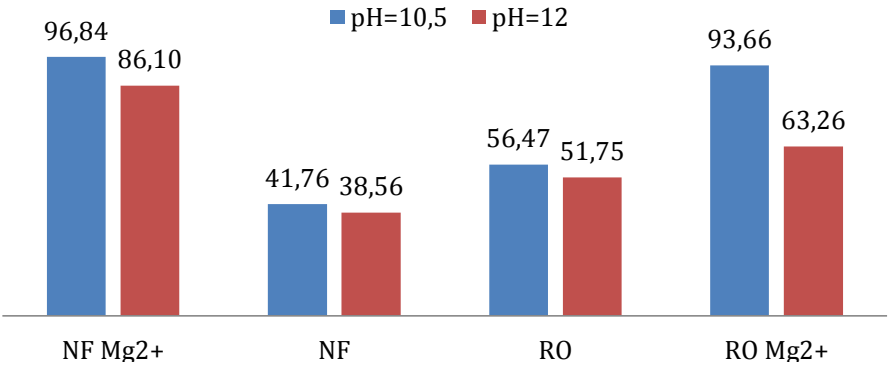

Figure 41. Effect of pH on the phosphate removal.

6.3.2.2. On the solid obtained

At pH=12, the Mg^{2+} in the reactor solution is maintained inexistent, as it precipitates directly when pumped into the reactor, leaving no amount in the solution (experiments 5 and 8). This is not observed when pH=10.5, as Mg^{2+} increases in the solution with time (experiments 1 and 4), (figure 42).

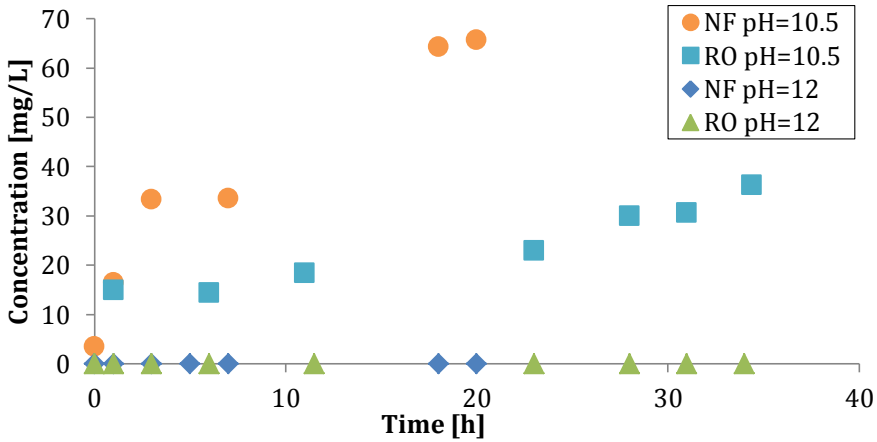

Figure 42. Mg^{2+} concentration with time.

This means that at pH=12, a Mg^{2+} salt precipitation is intensified in comparison with pH=10.5. The amount of solid obtained corroborates this: at pH 12 there is a bigger amount when there is Mg^{2+} (figure 43). This is due to the precipitation of a magnesium phosphate, which makes both phosphate and magnesium ions to diminish in the solution.

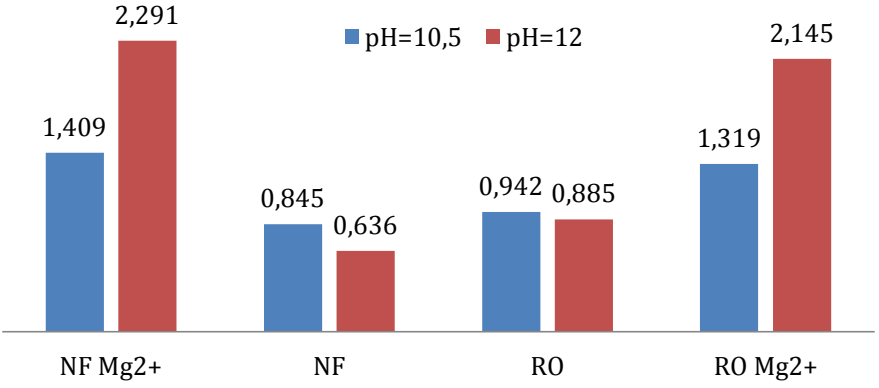

Figure 43. Effect of pH on the amount of solid obtained.

Hydroxyapatite is detected at both pH=10.5 and pH=12, indicating that both levels of alkalinity permit its formation.

6.3.3. Effect of the type of brine

As shown in (figure 44), NF at pH=10.5 with Mg^{2+} and its equal with RO brine arrive to a similar phosphate concentration in the remaining solution. In less time, NF brine removes the same amount of phosphate from the solution than RO. Without Mg^{2+} is slightly different: RO can remove the same phosphate than NF brine at 20 h, achieving higher % phosphate removal at 34 h.

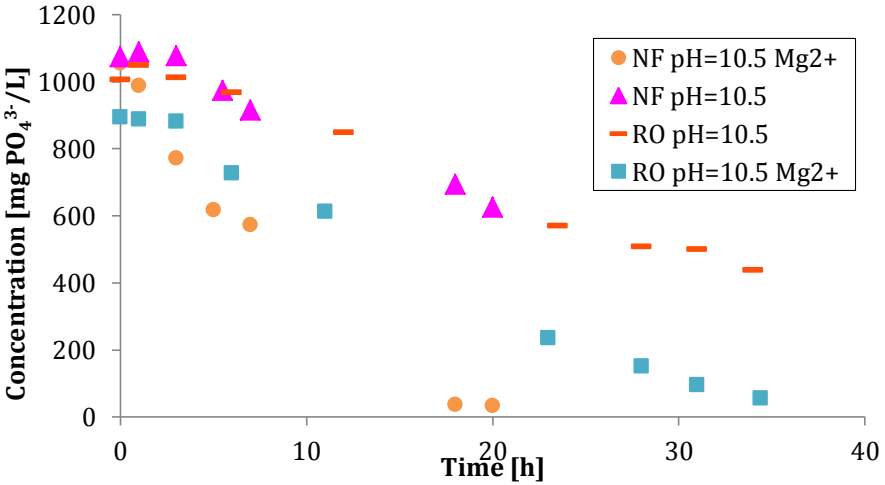

Figure 44. Phosphate concentration with time. Type of brine comparative.

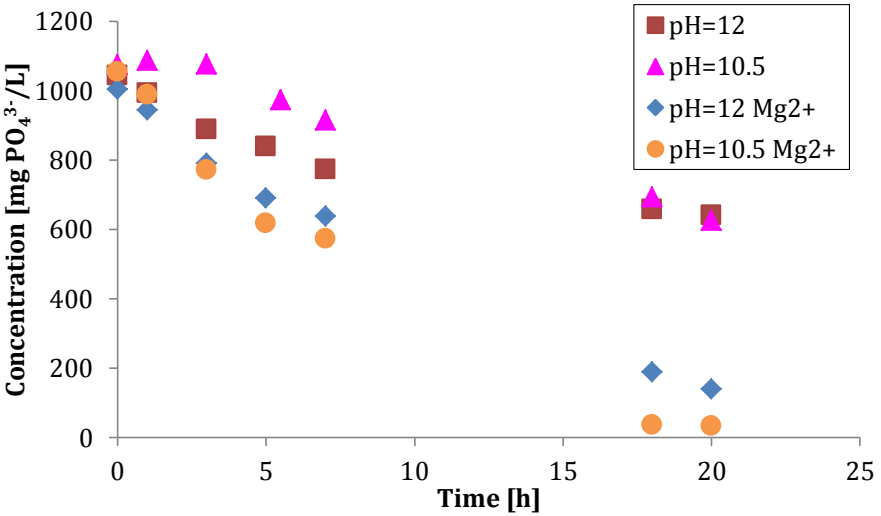

Figure 45. Phosphate concentration with time. NF brine.

When using nanofiltration brines, Mg^{2+} causes an accused decreasing curve, while the precipitation takes place at a slower path when this cation is not present (see figure 45). Therefore, at the same reaction time, higher % phosphate removal is achieved. Both types of brine are equally affected by the presence of Mg^{2+} and pH.

In short, the type of brine does not have a determining effect on the phosphate removal, as seen in figure 46.

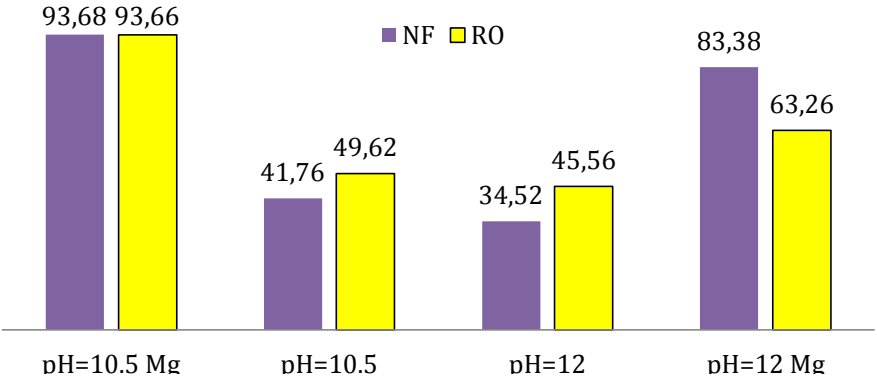

Figure 46. Effect of the type of brine on the phosphate removal.

Hydroxyapatite has been found on both types of brines, indicating that it can be formed in presence of other ions apart from Cl^-, obtaining a positive answer to the initial hypothesis.

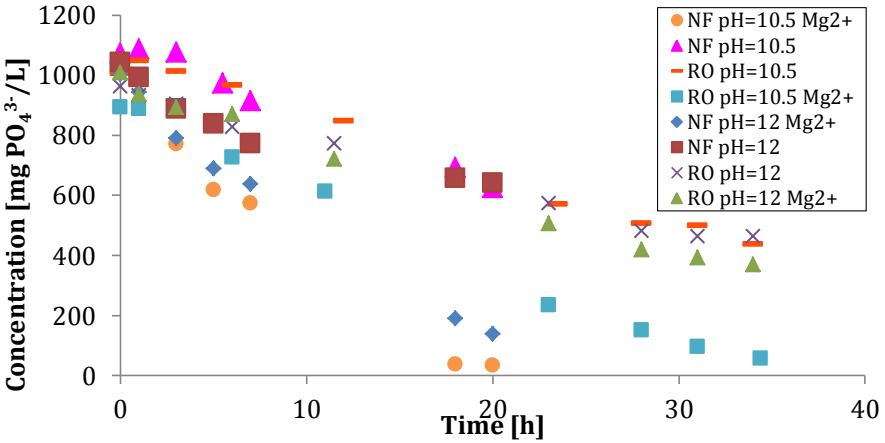

Figure 47. Global view of phosphate removal.

Figure 47 offers a global view of the phosphate decrease in all the experiments.

To summarise, the type of brine does not have as much effect as other factors, as Mg^{2+} presence or pH. As expected, results corroborate that Mg^{2+} cannot be found in the reactor when it is not present in the used brine (experiments 2, 3, 6 and 7).

7. CONCLUSIONS AND RECOMMENDATIONS

Phosphate removal was achieved by continuous chemical precipitation using a stirred batch reactor. The effects of certain parameters have been successfully determined, as well as the best conditions to obtain hydroxyapatite.

The presence of Mg^{2+} in the brine solution increases the amount of phosphate removed by precipitation, as well as the amount of solid obtained, as magnesium phosphate precipitates. Magnesium also affects the way phosphate is removed from the solution. The nucleation period is longer, and the concentration slope less abrupt when operating without magnesium.

In all four types of brines, higher removal is obtained at pH=10.5. The type of brine does not have as much effect as other factors such as the presence of Mg^{2+} or pH. In less time, NF brine removes the same amount of phosphate from the solution than RO brine when there is Mg^{2+}.

If the objective is to remove phosphate, the NF and RO brines with Mg^{2+} at pH=10.5 are the best options, representing almost a 100 % of removal.

Analyses conducted on solids have found the presence of spherical hydroxyapatite particles when using brines without magnesium, proving the hypothesis that HAP can be obtained in the presence of SO_4^{2-}, Na^+ and Cl^-. Slow and inefficient phosphate removal results in the formation of hydroxyapatite.

In conclusion, hydroxyapatite has been found at the two studied pH using both nanofiltration and reverse osmosis brines without magnesium.

Further studies could use real nanofiltration and reverse osmosis brines to check if it is possible to obtain a fertiliser by the precipitation of calcium phosphate. The phosphate source could be a synthetic solution as well but more diluted to simulate a less concentrated regenerated stream from the ion exchange unit. Investment on better and newer techniques for the determination of the solid obtained should allow the complete determination of the substances that form the precipitate.

8. REFERENCES AND NOTES

Bridger, G.L.; Salutsky, M.L., Starostka, R.W. (1962). Metal Ammonium Phosphates as Fertilizers, *Journal of Agricultural and Food Chemistry*, Vol.10 (3), pp.181-188.

Carpenter, S.R.; Caraco, N.F.; Smith, V.H. (1998). Nonpoint pollution of surface waters with phosphorus and nitrogen. *Ecological Applications*, Vol. 8, pp. 559–568.

Cordell, D.; Drangert, J.-O.; White, S. (2009). The story of phosphorus: global food security and food for thought. *Global Environmental Change*, Vol.19, pp. 292-305.

Donnert, D.; Salecker, M. (1999). Elimination of phosphorus from municipal and industrial waste water. *Water Science and Technology*, Vol. 40, pp. 195–202.

Fixen, P.E. (2009). World fertilizer nutrient reserves–a view to the future. *Better Crops With Plant Food*, Vol. 93, pp. 8-11.

Forster, C. (2003). Waste water treatment and technology. Thomas Telfort Publishing. ISBN 0-7277-3229-3.

Goloshchapov,D.L.; Kashkarov, V.M.; Rumyantseva, N.A.; Seredinn P.V.; Lenshin, A.S.; Agapov, B.L.; Domashevskaya, E.P. (2013). Synthesis of nanocrystalline hydroxyapatite by precipitation using hen's eggshell. *Ceramics International*, Vol. 39, pp. 4539–4549.

Greenwood, N.; Earnshaw, A. (1997). Chemistry of the Elements. Oxford:Butterworth-Heinemann (2nd Edn.) ISBN 0-7506-3365-4.

Kirkpatrick, B.; Fleming, L:E.; Squicciarini, D.; Backer, L.C.; Clark, R.; Abraham, W.; Benson, J.; Cheng, Y.S.; Johnson, D.; Pierce, R.; Zaias, J.; Bossart, G.D.; Baden, D.G. (2004). Literature Review of Florida Red Tide: Implications for Human Health Effects. *Harmful Algae*, Vol. 3, pp. 99-115.

Mobasherpour, I.; Soulati Heshajin, M.; Kazemzadeha, A.; Zakeri, M. (2007). Synthesis of nanocrystalline hydroxyapatite by using precipitation method. *Journal of Alloys and Compounds*, Vol. 430, pp. 330–333.

Ott, C.; Rechberger, H. (2012). The European phosphorus balance. *Resources, Conservation and Recycling*, Vol. 60, pp. 159–172.

Raynaud, S.; Champion E.; Bernache-Assollant, D.; Thomas P. (2002). Calcium phosphate apatite with variable Ca/P atomic ratio I. Synthesis, characterisation and thermal stability of powders. *Biomaterials*, Vol. 23, pp. 1065–1072.

Redfield, A.C. (1958). The biological control of chemical factors in the environment. *American Scientist*, Vol. 46, pp. 205–222.

Rivera-Muñoz, E.M.; Velázquez-Castillo, R.; Huirache-Acuña, R.; Cabrera-Torres, J.L.; Arenas-Alatorre, J. (2012). Synthesis and Characterization of Hydroxyapatite-Based Nanostructures: Nanoparticles, Nanoplates, Nanofibers and Nanoribbons. *Materials Science Forum,* Vol. 706 - 709, pp. 589-594.

Smit, A.L.; Bindraban, P.S.; Schroder, J.J.; Conijn, J.G.; van der Meer, H.G. (2009). Phosphorus in agriculture: global resources, trends and developments. Plant Research International, Waginen, The Netherlands. Report 282.

Wang, L.; Nancollas G.H. (2008). Calcium Orthophosphates: Crystallization and Dissolution. *Chemical Reviews*, Vol.108 (11), pp. 4628–69.

Wendling. L.A.; Blomberg, P.; Sarlin, T.; Priha, O.; Arnold, M. (2013). Phosphorus sorption and recovery using mineral-based materials: Sorption mechanisms and potential phytoavailability. *Applied Geochemistry*, Vol. 37, pp. 157-169.

9. ACRONYMS

In order of appearance:

HAP	Hydroxyapatite
WWTP	Waste Water Treatment Plant
mg	Miligram
PO_4^{3-}	Phosphate anion
L	Litre
mg PO_4^{3-}/L	Phosphate concentration
NF	Nanofiltration/Nanofiltració
RO	Reverse osmosis
Mg^{2+}	Magnesium cation. Oxidation state +2
pH	Power of hidrogen
EDAR	Estació Depuradora d'Aigües Residuals
OI	Osmosi inversa
P	Atomic phosphorus
ppm	Parts per million
kg	Kilogram
$Ca_5(PO_4)_3F$	Fluorapatite
$Ca_5(PO_4,CO_3)_3F$	Carbonate fluorapatite
P_2O_5	Phosphorus pentoxide
ha	Hectarea
N	Atomic nitrogen
Si	Atomic silicon
O_2	Oxigen gas

HABs	Harmful algal blooms
Fe	Atomic iron
Al	Atomic aluminium
Ca	Atomic calcium
$NH_4MgPO_4 \cdot 6H_2O$	Struvite
$Ca_5(PO_4)_3(OH)$	Hydroxyapatite
$Ca_{10}(PO_4)_6(OH)_2$	Hydroxyapatite. Crystal unit cell
Ca/P	Calcium to phosphate molar ratio
rpm	Revolutions per minute
mL	Mililitre
min	Minute
$CaCl_2$	Calcium chloride
M	Molar
g	Gram
Ca^{2+}	Calcium cation. Oxidation state +2
NaCl	Sodium chloride
$CaCl_2 \cdot H_2O$	Calcium chloride monohydrate
$NaHCO_3$	Sodium hydrogencarbonate
Na_2SO_4	Sodium sulphate
$MgCl_2 \cdot 6H_2O$	Magnesium chloride hexahydrate
h	Hour
mg	Miligram
XRD	X-ray diffraction
FTIR	Fourier Transform Infrared Spectrometer
FESEM	Field Emission Scanning Electron Microscope
EDS	Energy Dispersion Spectroscopy
µm	Micrometre

UV	Ultraviolet
nm	Nanometre
MSA	Methanesulphonic acid
ºC	Degree Celsius
Na^+	Sodium cation
Cl^-	Chloride anion
SO_4^{2-}	Sulphate anion
IR	Infrared
Pa	Pascal
BET	Brunauer-Emmett Teller
DLS	Dynamic Laser Scattering
DSC	Differential Scanning Calorimetry
Exp.	Experiment
cps	Intensity in counts/s
θ	Theta angle
º	Degree
ICDD	International Centre for Diffraction Data
cm^{-1}	Wavenumber
keV	KiloelectronVolts
S	Atomic sulphur
O	Atomic oxigen
C	Atomic carbon
$NaH_2PO_4 \cdot H_2O$	Sodium dihydrogen phosphate
NH_4VO_3	Ammonium metavanadate
$(NH_4)_6Mo_7O_{24} \cdot 4H_2O$	ammonium molybdate
HCl	hydrochloric acid
Na_2CO_3	Sodium carbonate

APPENDICES

APPENDIX 1: PREPARATION OF SOLUTIONS

In this appendix the methodology used for the preparation of different solutions in detailed.

10,000 ppm phosphate "mother" solution.

14.525 g of $NaH_2PO_4 \cdot H_2O$ are weighted in an analytical balance and dissolved in a 1 L volumetric flask with distilled water.

1,000 ppm phosphate solution.

25 mL and 50 mL volumetric flasks are filled with 10,000 ppm phosphate solution. Then, the 25 mL one is poured into a 250 mL one and filled with distilled water, and the same procedure with the 50 mL one into a 500 mL volumetric flask. At this point 750 mL of 1,000 ppm phosphate solution are prepared.

Vanadate-molybdate reagent. (According to Standard Methods for the determination of inorganic non-metals, 4500-P PHOSPHORUS, approved by Standard Methods Committee, 1999).

Two solutions must be prepared separately, named A and B. Solution B is to be prepared first. 1.25 g ammonium metavanadate NH_4VO_3 are dissolved in 300 mL distilled water contained in a 500 mL beaker by heating to boiling using a combined hot-plate magnetic-stirrer device. Once it is dissolved, the solution must be left to cool to room temperature. While this takes place, solution A is prepared dissolving 25 g of ammonium molybdate $(NH_4)_6Mo_7O_{24} \cdot 4H_2O$ in 300 mL distilled water, using a 500 mL beaker and a magnetic stirrer device. When solution B is cold, it is poured into a 1 L volumetric flask, and then added 330 mL of 37% hydrochloric acid HCl, working inside the fume cupboard. The 330 mL are measured using 100 mL, 25 mL and 5 mL volumetric flasks. The solution B is let to cool again, still inside the fume cupboard, and then solution A is poured into the 1 L volumetric flask where solution B is. Distilled water is added until 1 L is achieved and then mixed to guarantee homogeneity.

Chromatography eluents.

A cationic eluent and an anionic eluent are prepared to operate the chromatograph. To prepare the cationic eluent: dilute 3.9 mL of methanesulfonic acid into 2 L of distilled water using

a volumetric flask. To prepare the anionic eluent: dissolve 0.954 g of Na_2CO_3 in distilled water and then add 0.134 g of $NaHCO_3$ dissolve with distilled water in a 2 L volumetric flask.

APPENDIX 2: ANALYTICAL METHODS

In this appendix there are photographs of different analytical instruments used, accessories and manufacturer specifications.

Spectrophotometry

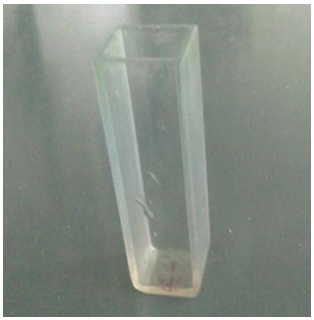

Figure 48. Quartz cuvette.

Figure 49. UV spectrometer.

Chromatography

Figure 50. Ion-exchange chromatography equipment.

Figure 51. AS40 automated sampler.

Figure 52. AS40 automated sampler sample container.

APPENDIX 3: SOLID CHARACTERISATION

SEM images

Different magnifications of the solids obtained are presented in the next images. The best micrographs have been selected to view the structure, and some experiments have more than one magnification to ensure a correct visualisation.

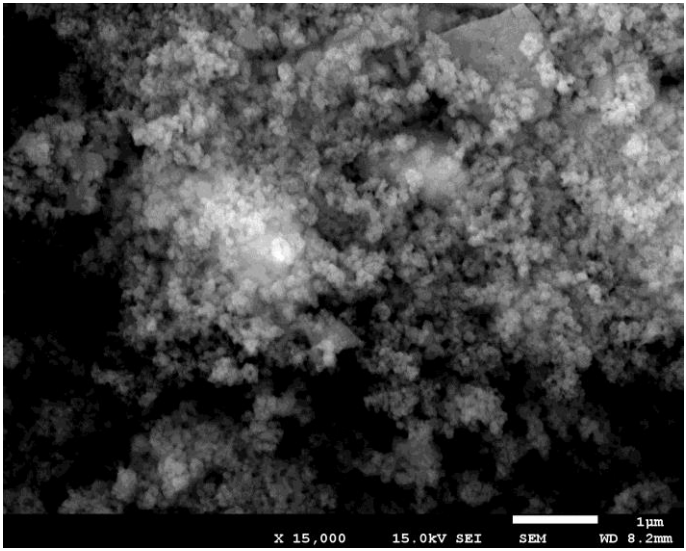

Figure 53. SEM micrograph (x 15,000 magnifications). Exp. 1. Nanofiltration brine (with Mg^{2+}) at pH=10.5.

Spherical particles can be identified in figure 53 with x 15,000 magnifications. A closer picture confirms the rounded particles (figure 54).

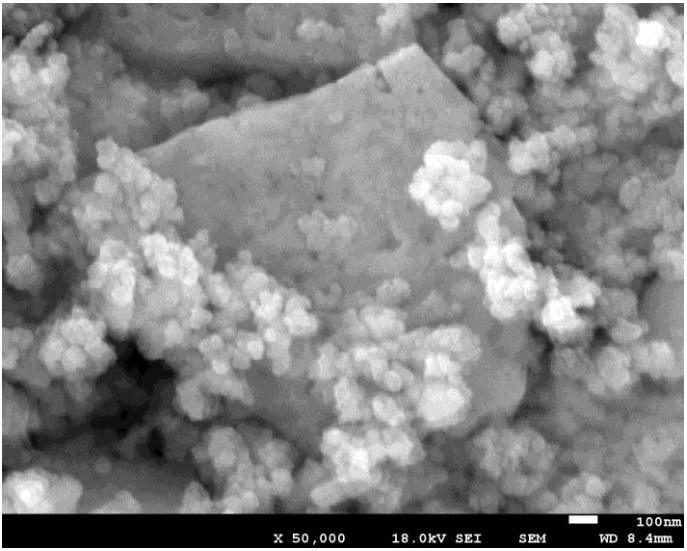

Figure 54. SEM micrograph (x 50,000 magnifications) Exp. 1. Nanofiltration brine (with Mg^{2+}) at pH=10.5.

Although XRD analysis did not found HAP, they could be repeated to verify that spoilage of the samples did not take place.

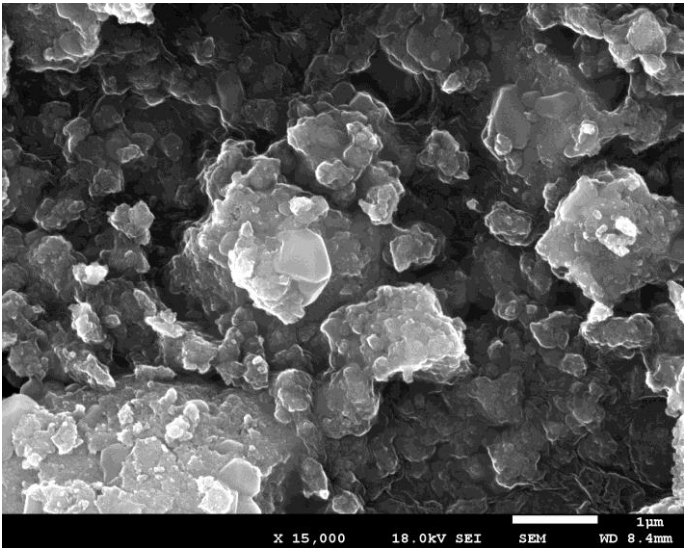

Figure 55. SEM micrograph (x 15,000 magnifications). Exp. 2. Nanofiltration brine at pH=10.5.

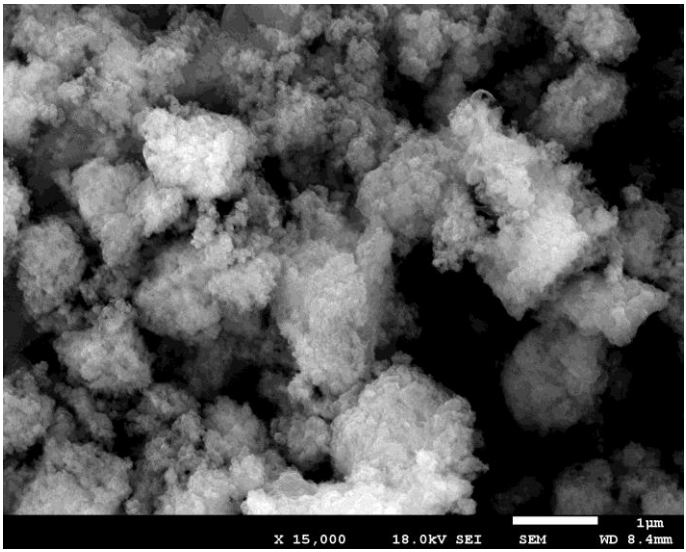

Figure 56. SEM micrograph (x 15,000 magnifications). Exp. 3. Reverse osmosis brine at pH=10.5.

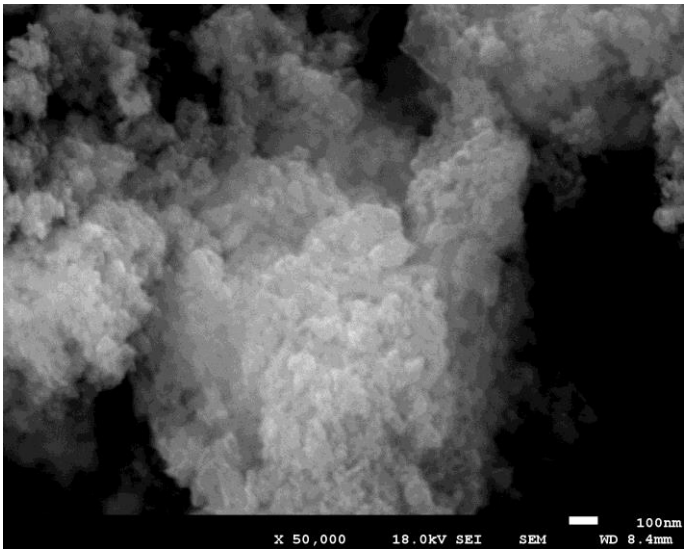

Figure 57. SEM micrograph (x 50,000 magnifications). Exp. 3. Reverse osmosis brine at pH=10.5.

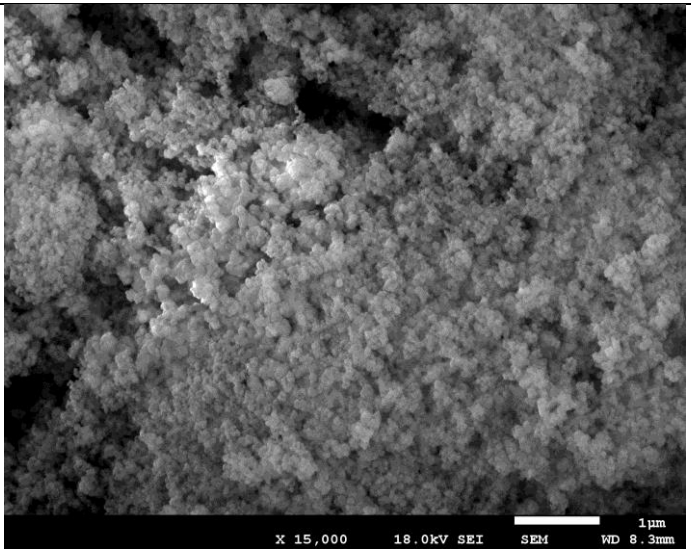

Figure 58. SEM micrograph (x 15,000 magnifications). Exp. 4. Reverse osmosis brine (with Mg^{2+}) at pH=10.5.

Spherical particles are also present in experiment 4 solid, as seen in pictures 58 and 59.

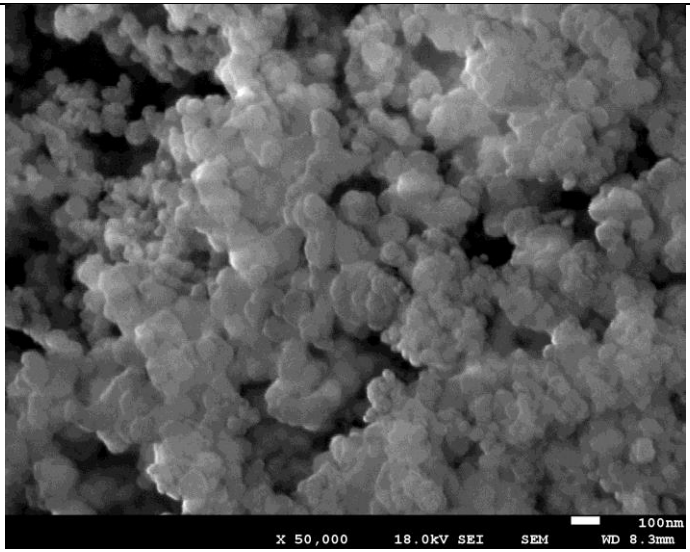

Figure 59. SEM micrograph (x 50,000 magnifications). Exp. 4. Reverse osmosis brine (with Mg^{2+}) at pH=10.5.

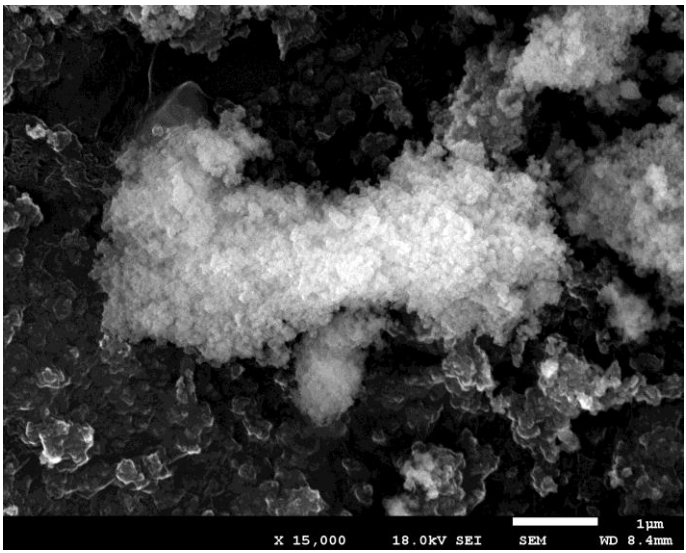

Figure 60. SEM micrograph (x 15,000 magnifications). Exp. 5. Nanofiltration brine (with Mg^{2+}) at pH=12.

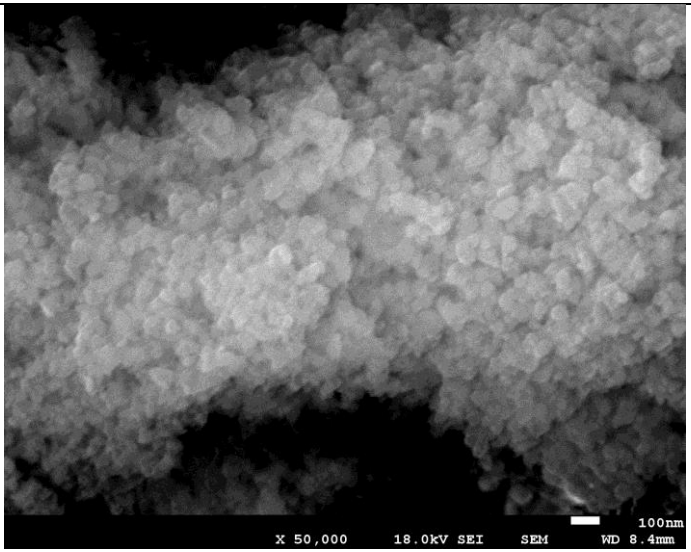

Figure 61. SEM micrograph (x 50,000 magnifications). Exp. 5. Nanofiltration brine (with Mg^{2+}) at pH=12.

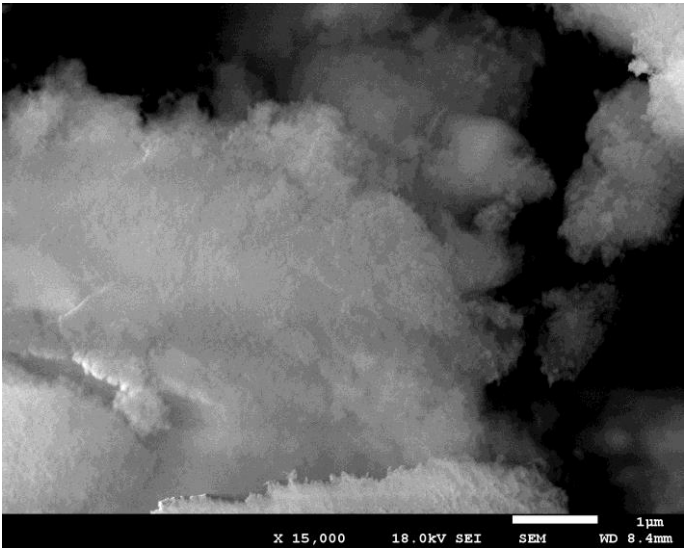

Figure 62. SEM micrograph (x 15,000 magnifications). Exp. 6. Nanofiltration brine at pH=12.

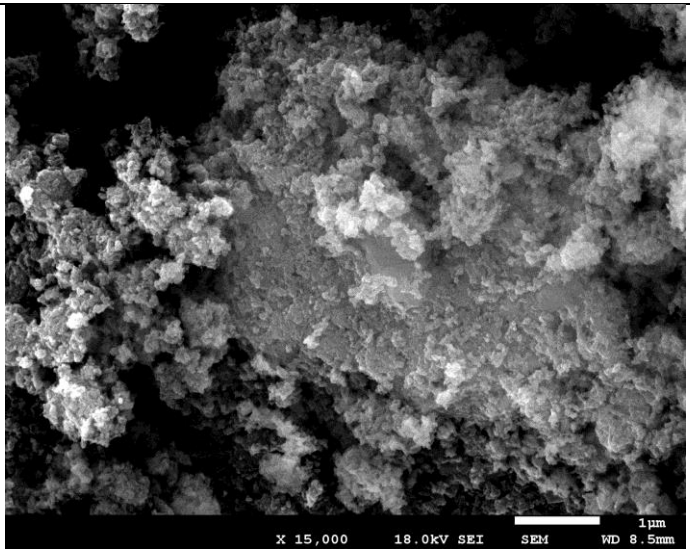

Figure 63. SEM micrograph (x 15,000 magnifications). Exp. 7. Reverse osmosis brine at pH=12.

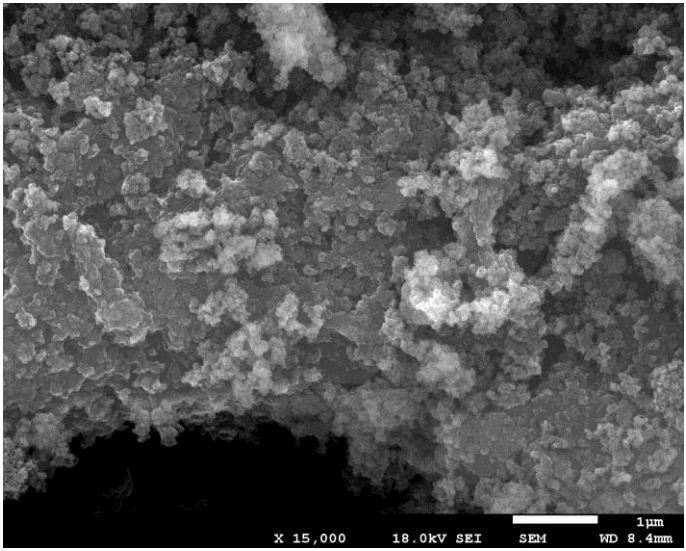

Figure 64. SEM micrograph (x 15,000 magnifications). Exp. 8. Reverse osmosis brine (with Mg^{2+}) at pH=12.

Equipment used

Photographs of the different equipment used for taking the micrographs of the solid.

Figure 65. Cressington Sputter Coater 208 HR.

Figure 66. Cressington Sputter Coater 208 HR (detail).

Figure 67. JEOL JSM-7001F Field Emission Scanning Electron Microscope.